NATIONAL AERONAUTICS AND SPACE ADMINISTRATION

Technical Report 32-1602

The Prediction of Zenith Range Refraction From Surface Measurements of Meteorological Parameters

JET PROPULSION LABORATORY
CALIFORNIA INSTITUTE OF TECHNOLOGY
PASADENA, CALIFORNIA

July 15, 1976

NATIONAL AERONAUTICS AND SPACE ADMINISTRATION

Technical Report 32-1602

The Prediction of Zenith Range Refraction From Surface Measurements of Meteorological Parameters

Allen L. Berman

JET PROPULSION LABORATORY
CALIFORNIA INSTITUTE OF TECHNOLOGY
PASADENA, CALIFORNIA

July 15, 1976

Preface

The work described in this report was performed by the DSN Operations Division of the Jet Propulsion Laboratory.

Acknowledgments

I would like to thank J. A. Wackley, who painstakingly proofed the document, L. Y. Lim, who graciously used MBASIC capabilities to compute and plot the various models in Appendix II, and R. B. Miller, who goaded me into publishing this material.

Contents

Tables

Figures

Abstract

This report presents the prediction of zenith range refraction from surface measurements of meteorological parameters. Refractivity is separated into wet (water vapor pressure) and dry (atmospheric pressure) components. The integration of dry refractivity is shown to be exact. Attempts to integrate wet refractivity directly prove ineffective; however, several empirical models developed by the author and other researchers at JPL are discussed. The best current wet refraction model is here considered to be a separate day/night model ("Berman (D/N)"), which is proportional to surface water vapor pressure and inversely proportional to surface temperature. The standard deviation of this model is considered to be:

$$\sigma \approx 1.5 - 2.0\,\text{cm}$$

Methods are suggested that might improve the accuracy of the wet range refraction model; however, the information content in surface parameters is considered insufficient to allow a surface measurements model for wet range refraction to result in a standard deviation lower than

$$\sigma \approx 1.0 - 1.5\,\text{cm}$$

The Prediction of Zenith Range Refraction From Surface Measurements of Meteorological Parameters

I. Introduction

In the last two decades, increasingly sophisticated deep space missions have placed correspondingly stringent requirements on navigational accuracy. As part of the effort to increase navigational accuracy, and hence the quality of radiometric data, much effort has been expended in an attempt to understand and compute the tropospheric effect on range (and hence range rate) data. The general approach adopted has been that of computing a zenith range refraction, and then mapping this refraction to any arbitrary elevation angle via an empirically derived function of elevation. Thus if

ΔR = zenith range refraction, cm

θ = elevation angle, deg

$f(\theta)$ = elevation "mapping" function

then

$$\Delta R_\theta = \Delta R \{f(\theta)\}$$

where

$$f(90) = 1$$

The relevant parameters necessary to the determination of tropospheric range refraction are as follows:

n = index of refraction

N = refractivity

z = height above station, km

r = range, km

r' = refracted range, km

c = speed of light, km/s

t = time, s

where

$$n = 1 + 10^{-6} N$$

One begins by considering the physical signal path range as the troposphere is traversed:

$$dt = \frac{dz}{c}$$

and

$$r = \int c dt = \int dz$$

One then considers an apparent refracted range r' ("signal retardation") with signal velocity v ($c > v$):

$$v = \frac{c}{n}$$

$$dt' = \frac{dz}{v}$$

and

$$r' = \int c\,dt' = \int c\frac{dz}{v} = \int n\,dz$$

so that the corresponding range refraction would be

$$\begin{aligned}\Delta R &= 10^6 [r' - r] \\ &= 10^6 [\int n\,dz - \int dz] \\ &= 10^6 \int (n-1)\,dz \\ &= 10^6 \int 10^{-6} N\,dz \\ &= 10^{-1} \int N\,dz\end{aligned}$$

Prior to 1970, attempts to calculate this quantity generally assumed that

$$N(z) = N_s \exp(-B_1 z)$$

where

N_s = surface refractivity

B_1 = "inverse scale height," km (≈ 0.1)

with B_1 an empirically determined constant. The total range refraction (considering that tropospheric type range refraction is nil by about 75 km) was then

$$\begin{aligned}\Delta R &= 10^{-1} \int_0^{75} N_s \exp(-B_1 z)\,dz \\ &\approx 10^{-1} \int_0^{\infty} N_s \exp(-B_1 z)\,dz \\ &= 10^{-1} \frac{N_s}{B_1}\end{aligned}$$

In 1970, this author broke new ground (Ref. 1) by considering the wet and dry components of refractivity separately, viz,

$$N = ND + NW$$

where

ND = "dry" refractivity

$$= C_1 \frac{P}{T}$$

NW = "wet" refractivity

$$= C_1 C_2 \left\{\frac{PW}{T^2}\right\}$$

and

$C_1 = 0.776$

$C_2 = 4810.0$

P = (total) atmospheric pressure, N/m² (1 mbar $= 10^2$ N/m²)

T = temperature, K

PW = water vapor pressure, N/m²

$$= 610\,\{RH\} \exp\left(\frac{AT - B}{T - C}\right)$$

RH = relative humidity (1.0 = 100%)

$A = 7.4475 \ln(10) = 17.1485$

$B = 2034.28 \ln(10) = 4684.1$

$C = 38.45$

At that time it was shown that the quantity:

$$\int_0^{\infty} ND(z)\,dz$$

could be integrated exactly, while the quantity

$$\int_0^{\infty} NW(z)\,dz$$

could be integrated approximately, which represented a considerable breakthrough since the dry component of refractivity contributes the vast bulk of the refractive effect, viz,

$$0.90 \lesssim \frac{\int_0^{\infty} ND(z)\,dz}{\int_0^{\infty} N(z)\,dz} \lesssim 0.99$$

and

$$0.01 \lesssim \frac{\int_0^\infty NW(z)\,dz}{\int_0^\infty N(z)\,dz} \lesssim 0.10$$

This report reviews the work leading to the exact integration of the dry component of refractivity (Section II), and then presents a theoretical integration of the wet component of refractivity, as well as more recent work by the author and other researchers in the field towards the refinement of an expression for wet refraction (Section III). Finally, Section IV presents a summary, and comments on future prospects for additional gains in accuracy in the determination of range refraction from the measurement of surface meteorological parameters.

II. Determination of Dry Zenith Range Refraction

Dry range refraction is given by the following expression:

$$\Delta R_d = 10^{-1}\int_0^\infty ND(z)\,dz$$

where

ΔR_d = "dry" range refraction, cm

In the following Subsections, it will be shown that different atmospheric assumptions all lead to the same results for the determination of dry range refraction.

A. Isothermal Atmosphere

As was mentioned in Section I, early attempts to integrate (total) refractivity assumed a refractivity profile of

$$N(z) = N_s \exp(-B_1 z)$$

If one limits the discussion to dry refractivity only, one finds that this assumption is identical to the assumption of an isothermal, or constant temperature, atmosphere. The definition of an isothermal atmosphere (see Ref. 2, p. 82) is as follows:

$$T(z) = T_s$$

$$P(z) = P_s \exp\left(-\frac{gz}{RT_s}\right)$$

where

T_s = surface temperature, K

P_s = surface pressure, N/m^2

g = gravitational acceleration, 980.6 cm/s^2

R = Perfect Gas Constant, 0.287 J/gK

$$\frac{g}{R} = 34.1 \text{ K/km}$$

Calculating dry range refraction, one would have

$$\Delta R_d = 10^{-1}\int_0^\infty ND(z)\,dz = 10^{-1}\int_0^\infty C_1 \frac{P(z)}{T(z)}\,dz$$

$$= 10^{-1}\int_0^\infty C_1 \frac{P_s \exp\left(-\frac{gz}{RT_s}\right)}{T_s}\,dz$$

$$= 10^{-1}C_1\frac{P_s}{T_s}\int_0^\infty \exp\left(-\frac{gz}{RT_s}\right)dz$$

$$= 10^{-1}C_1\frac{P_s}{T_s}\left[-\left(\frac{RT_s}{g}\right)\exp\left(-\frac{gz}{RT_s}\right)\right]_0^\infty$$

$$= 10^{-1}C_1 P_s\left(\frac{R}{g}\right)$$

which leads to the conclusion that zenith dry range refraction can be determined simply by measuring the surface pressure.

B. Standard Atmosphere

An isothermal atmosphere is a rather poor assumption, however; a much better idea would be to assume a standard atmosphere profile. For instance, a typical profile (see Ref. 2, pp. 82–85) for a station at a height h_0 above sea level would be a constant lapse rate atmosphere to 11 km, defined as follows:

$$0 \le z \le (11 - h_0)$$

$$T(z) = T_s - \gamma z$$

$$P(z) = P_s\left(\frac{T(z)}{T_s}\right)^{g/R\gamma}$$

γ = lapse rate, K/km

$$= \left(\frac{T_s - T_1}{11 - h_0}\right)$$

$T_1 = 216.65$ K

and an isothermal atmosphere from 11 km to 21 km, defined as follows:

$$(11 - h_0) \leq z \leq (21 - h_0)$$

$$T(z) = T_1$$

$$P(z) = P_s\left(\frac{T_1}{T_s}\right)^{g/R\gamma} \exp\left(-\frac{z - [11 - h_0]}{RT_1}\, g\right)$$

Using the above atmospheric model, the calculation of dry zenith range refraction proceeds as follows:

$$\Delta R_d = 10^{-1}\int_0^z ND(z)\,dz$$

$$= 10^{-1}\int_0^z C_1\left(\frac{P(z)}{T(z)}\right)dz$$

$$= \int_0^{11-h_0} 10^{-1}C_1\frac{P_s}{T_s}\left(\frac{T_s - \gamma z}{T_s}\right)^{\frac{g}{R\gamma}-1} dz$$

$$+ \int_{11-h_0}^{21-h_0} 10^{-1}C_1\frac{P_s}{T_1}\left(\frac{T_1}{T_s}\right)^{g/R\gamma}$$

$$\times \exp\left(-\frac{z - [11 - h_0]}{RT_1}\, g\right)dz$$

The upper limit of the second integral $(21 - h_0)$ is allowed to go to infinity (because of the small contribution above 21 km) so that

$$\Delta R_d \cong 10^{-1}C_1P_s\left\{\frac{1}{T_s}\int_0^{11-h_0}\left(\frac{T_s - \gamma z}{T_s}\right)^{\frac{g}{R\gamma}-1} dz\right.$$

$$\left. + \frac{1}{T_1}\int_{11-h_0}^{\infty}\left(\frac{T_1}{T_s}\right)^{g/R\gamma}\exp\left(-\frac{z - [11 - h_0]}{RT_1}\, g\right)dz\right\}$$

$$= 10^{-1}C_1P_s\left\{\frac{RT_s}{gT_s}\left[1 - \left(\frac{T_1}{T_s}\right)^{g/R\gamma}\right] + \frac{RT_1}{gT_1}\left(\frac{T_1}{T_s}\right)^{g/R\gamma}\right\}$$

$$= 10^{-1}C_1P_s\left(\frac{R}{g}\right)\left\{1 - \left(\frac{T_1}{T_s}\right)^{g/R\gamma} + \left(\frac{T_1}{T_s}\right)^{g/R\gamma}\right\}$$

$$= 10^{-1}C_1P_s\left(\frac{R}{g}\right)$$

which is, of course, identical to the result obtained for the previously considered isothermal atmosphere.

C. Hydrostatic Equation and the Perfect Gas Law

Finally, it can be quite easily shown that the above result can easily be obtained by merely assuming the hydrostatic equation and the perfect gas law:

$$dP = -\rho g\,dz \qquad \text{(hydrostatic equation)}$$

where:

ρ = density

and

$$P = \rho RT \qquad \text{(perfect gas law)}$$

One then has:

$$ND(z) = C_1\frac{P(z)}{T(z)} = C_1\frac{\rho RT(z)}{T(z)}$$

$$= C_1\rho R$$

$$= C_1\left(-\frac{1}{g}\left[\frac{dP}{dz}\right]\right)R$$

so that

$$\Delta R_d = 10^{-1}\int_0^z ND(z)\,dz$$

$$= -\frac{10^{-1}C_1}{g}\int_0^{\infty}\left(\frac{dP}{dz}\right)R\,dz$$

$$= -\frac{10^{-1}C_1R}{g}\int_{P_s}^{0} dP$$

or, once again,

$$= 10^{-1}C_1P_s\left(\frac{R}{g}\right)$$

the above results lead to the unmistakable conclusion that dry zenith range refraction is simply a linear function of surface pressure:

$$\Delta R_d = 10^{-1}C_1P_s\left(\frac{R}{g}\right)$$

and not of surface refractivity, as was formerly believed.

III. Determination of Wet Zenith Range Refraction

In the previous section, it was seen that for dry zenith range refraction one has:

$$\Delta R_d = 10^{-6} \int_0^\infty ND(z)\,dz$$

$$= 10^{-6} C_1 P_s \left(\frac{R}{g}\right)$$

Correspondingly in this section, the quantity of interest is wet zenith range refraction:

$$\Delta R_w = 10^{-6} \int_0^\infty NW(z)\,dz$$

or:

$$\Delta R_w = 10^{-6} \int_0^\infty C_1 C_2 \frac{P_w(z)}{[T(z)]^2}\,dz$$

where:

$$P_w(z) = 610\, RH(z) \exp\left(\frac{AT(z) - B}{T(z) - C}\right)$$

Obviously, before one can attempt the determination of the integral of wet refractivity, one must know something about the functional dependence of temperature and relative humidity upon height above the station (z). Subsection III-A below will describe typical temperature and relative humidity (altitude) profiles, while Subsection III-B will present an integration of wet refractivity based on several simplifying assumptions. Subsections III-C and III-D present expressions for wet range refraction as derived by C. C. Chao and P. S. Callahan at the Jet Propulsion Laboratory in 1973. Subsection III-E presents more recent work (1974) by Berman on wet zenith range refraction, while Subsection III-F compares the expressions for wet zenith range refraction derived in Subsections III-B through III-E.

A. Temperature and Relative Humidity Profiles

The functional dependence of temperature and relative humidity upon altitude obeys no simple laws that would lead to convenient, explicit expressions for $T(z)$ and $RH(z)$; about the best one could expect to accomplish would be to find the best approximations for $T(z)$ and $RH(z)$ that are not so cumbersome or restrictive that they effectively preclude their usage for the purposes intended here. A brief description of temperature and relative humidity profiles ensues.

1. Temperature profiles. The region of interest in defining the functional dependence of temperature upon altitude is from the station height to the tropopause, or roughly 0 to 11 km. At the tropopause, the temperature is approximately −55°C, and at this temperature wet refractivity is nil. It is fortunate that many of the Deep Space Stations (DSS) are meteorologically similar, i.e., temperate, semiarid, and not in proximity to any large bodies of water. For climates such as these, one can identify two basic types of temperature profiles: a summer-type profile (warm and usually clear), and a winter-type profile (cold and often cloudy). The summer-type profile is the simpler of the two, and is shown in Fig. 1.

Generally, over a period of days, the temperature lapse rate and T_x ("extrapolated surface temperature") remain reasonably constant, although near the ground there is a diurnal swing from night inversion to day ground heating, and back. The winter-type profiles are more complicated in that inversions occur up to a far greater altitude, and rather than one main segment, they consist of several segments, as seen in Fig. 2.

To formulate a general expression for $T(z)$, which would account for the local surface effects, would be an almost impossible task; however, if one could extrapolate the temperature lapse rate down to the surface and define an "extrapolated surface temperature (T_x)," one could

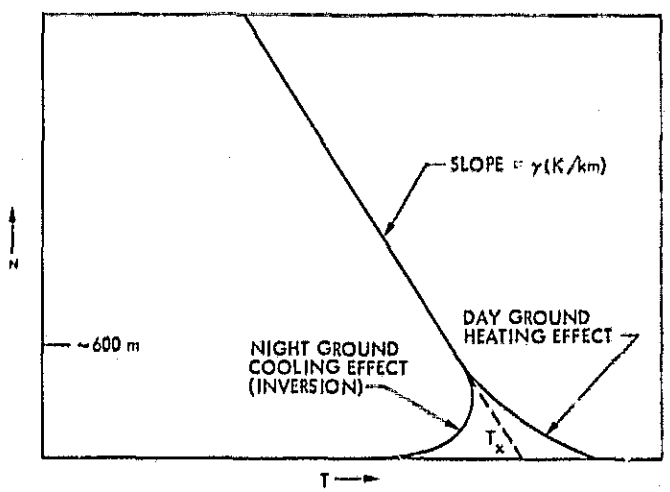

Fig. 1. Summer type profile

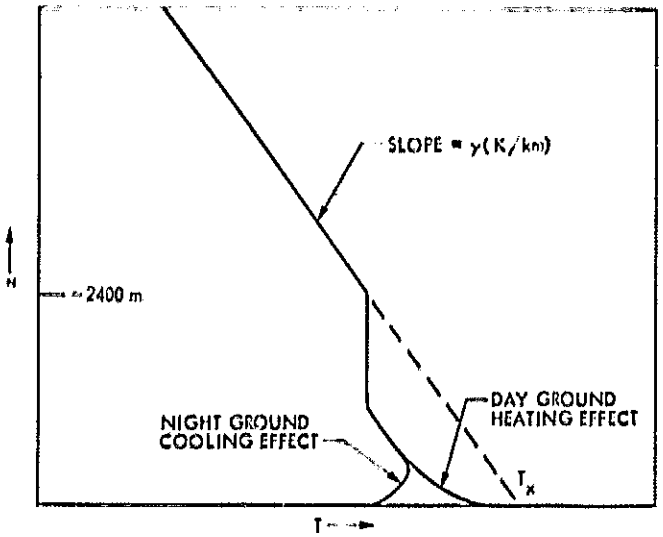

Fig. 2. Winter type profile

easily construct a simple general function of temperature up to the tropopause, as follows:

$$T_x = \text{extrapolated surface temperature}$$

$$T(z) = T_x - \gamma z$$

$$\gamma(T_x, h_0) = \left\{\frac{T_x - T_1}{11 - h_0}\right\}$$

This approximation should work reasonably well for summer-type profiles, but less well for winter-type profiles; however, the summer wet range refraction values are frequently 5 or more times the size of winter wet range refraction values, so at least the approximation would be most accurate when range refraction is at its largest.

2. Relative humidity profiles. After examining a number of relative humidity profiles, one is forced to conclude that there appears to exist no particular functional dependence of relative humidity upon height above the station (such as exists with temperature); perhaps the most that can be inferred is that relative humidity seems (but only tenuously!) to remain more constant with altitude during summer-type weather than during winter-type weather—although this would once again have a good implication in the far larger magnitude of summer range refraction values as compared to winter range refraction values. Some typical examples of relative humidity profiles are shown in Fig. 3.

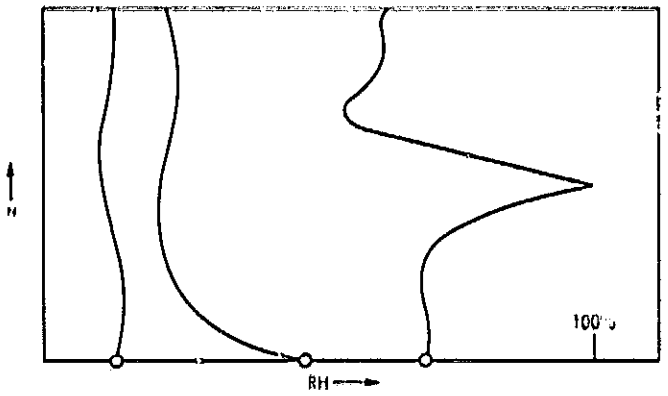

Fig. 3. Relative humidity profiles

Since no patterns are really discernable, one might advantageously assume:

$$RH(z) \sim \text{constant}$$

and since the greatest contribution to wet range refraction occurs near the surface, where:

$$RH(0) = RH_s$$

and

$$RH_s = \text{surface relative humidity}$$

it would seem appropriate to allow:

$$RH(z) = RH_s$$

3. Actual temperature and relative humidity profiles. Appendix A presents 10 actual temperature and relative humidity profiles measured at Edwards Air Force Base during 1968–1969. The profiles are alternate day–night cases, and were chosen during the following months:

(1) December

(2) February

(3) April

(4) August

(5) September

to provide seasonal variation. These cases will be utilized to test the various hypotheses advanced in the pursuit of a wet range refraction model, as detailed in the subsections that follow.

B. Direct Integration of Wet Zenith Refractivity

In Subsection A, expressions for $T(z)$ and $RH(z)$ were postulated as follows:

$$T(z) = T_s - \gamma z$$

where:

T_s = extrapolated surface temperature

$$\gamma = \left\{\frac{T_s - T_1}{11 - h_0}\right\}$$

and

$$RH(z) = RH_s$$

Assuming wet refractivity is nil by the tropopause, the integral one wishes to evaluate is:

$$\Delta R_w = 10^{-6} C_1 C_3 \int_0^{11} \frac{P_w(z)}{[T(z)]^2}\, dz$$

and since:

$$P_w(z) = 610\, RH(z) \exp\left(\frac{AT(z) - B}{T(z) - C}\right)$$

then:

$$\Delta R_w = 10^{-6} C_1 C_2 \int_0^{11} \frac{RH(z)}{[T(z)]^2} \exp\left(\frac{AT(z) - B}{T(z) - C}\right) dz$$

where

$$C_2 = 610\, C_3 = 2934100$$

Now since

$$RH(z) = RH_s$$

then

$$\Delta R_w = 10^{-6} C_1 C_2 RH_s \int_0^{11} \frac{1}{[T(z)]^2} \exp\left(\frac{AT(z) - B}{T(z) - C}\right) dz$$

Finally, utilizing

$$T(z) = T_s - \gamma z$$
$$dT = -\gamma\, dz$$

one has

$$\Delta R_w = 10^{-6} C_1 C_2 RH_s \int_{T_s}^{T_1} \frac{1}{T^2} \left\{\exp\left(\frac{AT - B}{T - C}\right)\right\} \left[-\frac{dT}{\gamma}\right]$$

$$= \left\{-\frac{10^{-6} C_1 C_2 RH_s}{\gamma}\right\} \int_{T_s}^{T_1} \frac{1}{T^2} \left\{\exp\left(\frac{AT - B}{T - C}\right)\right\} dT$$

thus one wishes to evaluate the integral

$$W(T_s) = \int_{T_s}^{T_1} \exp\left(\frac{AT - B}{T - C}\right) \frac{dT}{T^2}$$

If the substitution

$$Y = \frac{AC - B}{T - C}$$

is made, one then has

$$\exp\left(\frac{AT - B}{T - C}\right) = \exp(A + Y)$$
$$= \exp(A) \exp(Y)$$

and

$$T = \frac{AC - B + CY}{Y}$$

$$dT = \frac{B - AC}{Y^2}\, dY$$

$$\frac{dT}{T^2} = \frac{B - AC}{Y^2}\, dY \left[\frac{Y^2}{(AC - B + CY)^2}\right]$$

If one defines

$$Y_0 = \frac{AC - B}{C}$$

then

$$\frac{dT}{T^2} = \frac{1}{B - AC} \left[\frac{dY}{(1 + Y/Y_0)^2}\right]$$

so that

$$W(T_s) = \int_{T_s}^{T_0} \exp\left(\frac{AT - B}{T - C}\right)\frac{dT}{T^2} = \frac{\exp(A)}{B - AC}\int_{Y(T_s)}^{Y(T_0)} \frac{\exp(Y)}{(1 + Y/Y_0)^2}\,dY$$

For the most extreme possible range of temperatures, one has for the variation in the Y-dependent terms

$$216 \lesssim T \lesssim 316$$
$$-22.7 \lesssim Y \lesssim -14.5$$
$$1.4 \times 10^{-10} \lesssim \exp(Y) \lesssim 5 \times 10^{-7}$$
$$1.15 \lesssim (1 + Y/Y_0) \lesssim 1.22$$

since the variation in the denominator is almost nil compared to the variation in the exponential term, one might guess that an approximate solution could be of the form

$$\int \frac{\exp(Y)}{(1 + Y/Y_0)^2}\,dY \sim \frac{\exp(Y)}{(1 + Y/Y_0)^2}$$

This motivates an attempt to determine a solution by first assuming that

$$\int \frac{\exp(Y)}{(1 + Y/Y_0)^2}\,dY = \frac{\exp(Y)}{(1 + Y/Y_0)^2}F(Y)$$

and then attempting to solve the resultant differential equation in $F(Y)$. One begins by differentiating both sides:

$$\frac{\exp(Y)}{(1 + Y/Y_0)^2} = \frac{\exp(Y)}{(1 + Y/Y_0)^2}F(Y) - \left(\frac{2}{Y_0}\right)\frac{\exp(Y)}{(1 + Y/Y_0)^3}F(Y) + \frac{\exp(Y)}{(1 + Y/Y_0)^2}\frac{dF(Y)}{dY}$$

so that

$$1 = F(Y) - \left(\frac{2}{Y_0}\right)\frac{F(Y)}{(1 + Y/Y_0)} + \frac{dF(Y)}{dY}$$

or

$$\frac{dF(Y)}{dY} + F(Y)\left\{1 - \left(\frac{2}{Y_0}\right)\frac{1}{(1 + Y/Y_0)}\right\} - 1 = 0$$

An asymptotic series solution is postulated as follows:

$$F(Y) = \sum_{j=0}^{\infty}\frac{A_j}{(1 + Y/Y_0)^j}$$

$$\frac{dF(Y)}{dY} = \sum_{j=0}^{\infty}\frac{A_j}{(1 + Y/Y_0)^{j+1}}\left(-j\right)\left(\frac{1}{Y_0}\right) = -\sum_{j=0}^{\infty}\left(\frac{j}{Y_0}\right)\frac{A_j}{(1 + Y/Y_0)^{j+1}}$$

To deduce a recursion relationship, the terms in $F(Y)$ are manipulated:

$$F(Y) = \sum_{j=0}^{\infty}\frac{A_j}{(1 + Y/Y_0)^j} = A_0 + \sum_{j=1}^{\infty}\frac{A_j}{(1 + Y/Y_0)^j} = A_0 + \sum_{j=0}^{\infty}\frac{A_{j+1}}{(1 + Y/Y_0)^{j+1}}$$

and

$$-\left(\frac{2}{Y_0}\right)\frac{1}{(1 + Y/Y_0)}F(Y) = -\left(\frac{2}{Y_0}\right)\frac{1}{(1 + Y/Y_0)}\sum_{j=0}^{\infty}\frac{A_j}{(1 + Y/Y_0)^j} = -\left(\frac{2}{Y_0}\right)\sum_{j=0}^{\infty}\frac{A_j}{(1 + Y/Y_0)^{j+1}}$$

so that

$$-\sum_{j=0}^{\infty}\left(\frac{j}{Y_0}\right)\frac{A_j}{(1 + Y/Y_0)^{j+1}} + A_0 + \sum_{j=0}^{\infty}\frac{A_{j+1}}{(1 + Y/Y_0)^{j+1}} - \left(\frac{2}{Y_0}\right)\sum_{j=0}^{\infty}\frac{A_j}{(1 + Y/Y_0)^{j+1}} - 1 = 0$$

which requires

$$A_0 = 1$$

and

$$\sum_{j=0}^{\infty}\left\{\frac{A_{j+1}}{(1+Y/Y_0)^{j+1}}-\left(\frac{2}{Y_0}\right)\frac{A_j}{(1+Y/Y_0)^{j+1}}-\left(\frac{j}{Y_0}\right)\frac{A_j}{(1+Y/Y_0)^{j+1}}\right\}=0$$

so that

$$A_{j+1}-\left(\frac{2}{Y_0}\right)A_j-\left(\frac{j}{Y_0}\right)A_j=0$$

or

$$A_{j+1}=A_j\left\{\frac{2+j}{Y_0}\right\}$$

Combining $A_0=1$ and the above recursive relationship, one has

$$A_0=1$$

$$A_1=\frac{2}{Y_0}$$

$$A_2=\left(\frac{2}{Y_0}\right)\left(\frac{3}{Y_0}\right)$$

$$A_3=\left(\frac{2}{Y_0}\right)\left(\frac{3}{Y_0}\right)\left(\frac{4}{Y_0}\right)$$

$$\vdots$$

$$A_j=\frac{(j+1)!}{(Y_0)^j}$$

with the final result that

$$F(Y)=\sum_{j=0}^{\infty}\frac{(j+1)!}{(Y_0)^j(1+Y/Y_0)^j}$$

and

$$\int\frac{\exp(Y)}{(1+Y/Y_0)^2}\,dY=\frac{\exp(Y)}{(1+Y/Y_0)^2}\sum_{j=0}^{\infty}\frac{(j+1)!}{(Y_0)^j(1+Y/Y_0)^j}$$

Now the series

$$\sum_{j=0}^{\infty}\frac{(j+1)!}{(Y_0)^j(1+Y/Y_0)^j}$$

diverges as $j\to\infty$, viz:

$$\frac{(j+1)^{\text{th}}\text{ term}}{(j)^{\text{th}}\text{ term}}=\frac{(j+2)!(Y_0)^j(1+Y/Y_0)^j}{(Y_0)^{j+1}(1+Y/Y_0)^{j+1}(j+1)!}=\frac{j+2}{Y_0(1+Y/Y_0)}$$

and

$$\left|\frac{j+2}{Y_0(1+Y/Y_0)}\right|>1\text{ when }|j+2|>|Y_0+Y|$$

However, a solution is still valid for this asymptotic series as it converges very rapidly for small j:

$$j=0\text{ term}=1$$

$$j=1\text{ term}=\frac{2}{Y_0(1+Y/Y_0)}\approx-0.02$$

$$j=2\text{ term}=\frac{3\cdot 2}{(Y_0)^2(1+Y/Y_0)^2}\approx+0.006$$

so that

$$\int\frac{\exp(Y)}{(1+Y/Y_0)^2}\,dY=\frac{\exp(Y)}{(1+Y/Y_0)^2}\left\{1+\frac{2!}{Y_0(1+Y/Y_0)}+\frac{3!}{(Y_0)^2(1+Y/Y_0)^2}+\cdots\right\}$$

or

$$\int\frac{\exp(Y)}{(1+Y/Y_0)^2}\,dY\approx\frac{\exp(Y)}{(1+Y/Y_0)^2}$$

The final derived expression for wet zenith range refraction then becomes

$$\Delta R_w=\left\{-\frac{10^{-1}C_1C_2RH_s}{\gamma}\right\}W(T_s)$$

$$=\left\{-\frac{10^{-1}C_1C_2RH_s}{\gamma}\right\}\int_{T_s}^{T_1}\frac{1}{T^2}\left\{\exp\left(\frac{AT-B}{T-C}\right)\right\}dT$$

$$=\left\{-\frac{10^{-1}C_1C_2RH_s\exp(A)}{\gamma(B-AC)}\right\}\int_{Y(T_s)}^{Y(T_1)}\frac{\exp(Y)}{(1+Y/Y_0)^2}\,dY$$

$$=\left\{-\frac{10^{-1}C_1C_2RH_s\exp(A)}{\gamma(B-AC)}\right\}\frac{\exp(Y)}{1+Y/Y_0)^2}\Bigg|_{Y(T_s)}^{Y(T_1)}$$

and since

$$\frac{\exp\,[Y(T_1)]}{\exp\,[Y(T_s)]} \approx 3 \times 10^{-4}$$

one can ignore the upper limit, so that

$$\Delta R_w = \left\{\frac{10^{-6} C_1 C_2 R H_s \exp\,(A)}{\gamma(B - AC)}\right\} \frac{\exp\,[Y(T_s)]}{[1 + Y(T_s)/Y_0]^2}$$

Now

$$\exp\,(A) \exp\,[Y(T_s)] = \exp\left(\frac{AT_s - B}{T_s - C}\right)$$

and

$$[1 + Y(T_s)/Y_0]^2 = \left\{\frac{T_s}{T_s - C}\right\}^2$$

with the final result that

$$\Delta R_w = \left\{\frac{10^{-6} C_1 C_2 R H_s}{\gamma(B - AC)}\right\} \left[\left(1 - \frac{C}{T_s}\right)^2\right] \exp\left(\frac{AT_s - B}{T_s - C}\right)$$

The ten cases listed in Appendix A were numerically integrated (from this point on to be defined as the "actual") and compared to values computed from the above equation (now to be defined as the "Berman 70"). The results are seen in Table 1.

Table 1. Berman 70 vs Actual

Case No.	Berman 70, cm	Actual, cm	Δ, cm
Night cases			
1	13.3	4.8	+8.5
3	11.9	3.8	+8.1
5	5.3	3.7	+1.6
7	21.0	18.1	+2.9
9	10.8	9.7	+1.1
Day cases			
2	3.7	4.6	−0.9
4	4.5	2.9	+1.6
6	3.5	4.6	−1.1
8	17.0	19.3	−2.3
10	5.4	5.7	−0.3

The statistics of Table 1 above are as follows:

$$\sigma_{\text{night}} = 5.5 \text{ cm}$$

$$\sigma_{\text{day}} = 1.4 \text{ cm}$$

$$\sigma_{\text{total}} = 4.0 \text{ cm}$$

$$\text{bias}_{\text{night}} = +4.4 \text{ cm}$$

$$\text{bias}_{\text{day}} = -0.6 \text{ cm}$$

Although this model works reasonably well for the day cases, it is obvious that the combination of strong nighttime temperature inversion and ground distortion of (an increase in) relative humidity causes the model to be ineffective for night cases. Considering the composite $\sigma = 4.0$ cm, one would be better off using monthly averages (and with far less trouble!) of ΔR_w than one would be using this model, according to the work of V. J. Ondrasik and K. L. Thuleen on usage of monthly wet refraction averages (see Refs. 3 and 4). As a sidelight, however, S. C. Wu (Ref. 5) has been successful in applying the model above 3,000 m, which is quite reasonable in view of the fact that it is the near surface distortions in temperature and relative humidity that make the model ineffective for surface measurements.

C. The Chao Model

In 1973, C. C. Chao produced the following model ("Chao") to predict wet zenith range refraction (see Ref. 6):

$$\Delta R_w = 163 \frac{(PW_s)^{1.23}}{T_s^2} + 205\gamma \frac{(PW_s)^{1.46}}{T_s^3}$$

Chao began by assuming the following:

$$\frac{d}{dz}[PW] = -[\rho w]g; \qquad \text{hydrostatic equation}$$

$$PW = \rho w[RW]T; \qquad \text{perfect gas law}$$

$$T = T_s - \gamma z; \qquad \text{temperature lapse}$$

where

ρw = water vapor density

RW = perfect gas constant for water vapor

The above three equations led to unreasonable results, however, and Chao, considering the perfect gas law inapplicable, replaced it with the adiabatic law:

$$PW = K^{\beta}[\rho w]^{\beta}$$

where

β = specific heat ratio ($\sim$1.3 for water vapor)

In actual fact, there is no reason to question the adequacy of the perfect gas law for water vapor so long as condensation does not occur. As P. S. Callahan quite correctly pointed out (see Ref. 7), the real problem lies with a misapplication of the hydrostatic equation. For a mixture of gases, Dalton's Law (see Ref. 2, p. 18) states that the total pressure P is equal to the sum of the partial pressures of each constituent gas (j):

$$P = \sum_{j=0}^{i} P_j$$

so that for the atmosphere, the hydrostatic equation is

$$\frac{d}{dz}\left[\sum_{j=0}^{i} P_j\right] = -\rho^* g$$

with

ρ^* = weighted density

but it is not necessary that for each individual constituent gas

$$\frac{d}{dz}[P_j] = -\rho_j g$$

particularly in the case of water vapor, which (relatively speaking) has a very low saturation vapor pressure and is immensely affected by local surface effects, i.e., bodies of water, etc. Although the derivation of the model was flawed, the use of a constant parameter to fit actual data gave the model validity, and, in fact, it represented quite an improvement over the only other surface wet model then existent (Berman 70). Table 2 presents a comparison of the Chao model with the data for the ten test cases in Appendix A.

Table 2. Chao vs Actual

Case No.	Chao, cm	Actual, cm	Δ, cm
Night cases			
1	2.4	4.8	−2.4
3	2.7	3.8	−1.1
5	2.0	3.7	−1.7
7	14.7	18.1	−3.4
9	3.3	9.7	−6.4
Day cases			
2	1.5	4.6	−3.1
4	2.4	2.9	−0.5
6	3.6	4.6	−1.0
8	21.9	19.3	+2.6
10	5.1	5.7	−0.6

The statistics from Table 2 are as follows:

$$\sigma_{night} = 3.5 \text{ cm}$$

$$\sigma_{day} = 1.9 \text{ cm}$$

$$\sigma_{total} = 2.8 \text{ cm}$$

$$\text{bias}_{night} = -3.0 \text{ cm}$$

$$\text{bias}_{day} = -0.5 \text{ cm}$$

These can be compared to Chao's own published figures (from Ref. 6):

$$\sigma_{night} = 4.1 \text{ cm}$$

$$\sigma_{day} = 2.0 \text{ cm}$$

The performance of the model in regard to day cases is creditable, although even the day residuals appear to have a definite negative bias; for instance, in Fig. 4, p. 41, of Ref. 6, 17 of 19 day case residuals are negative. For night cases, however, the model does poorly; even more troublesome than the relatively large standard deviation is the very large negative bias (−3 cm). This very large night case bias is likewise readily seen in the same Fig. 4, Ref. 6. The overall performance of the Chao model will be compared to other models in Subsection III-F.

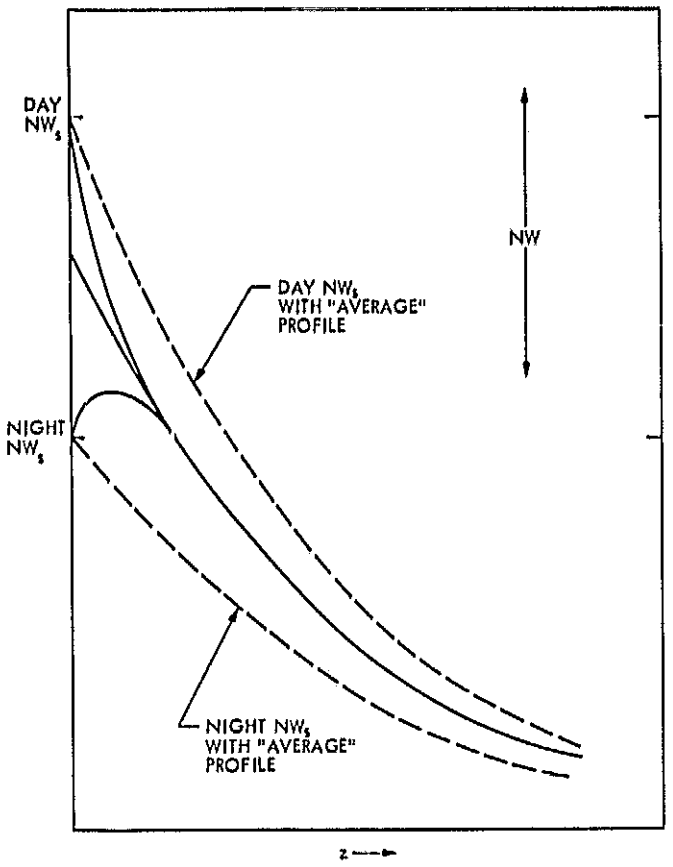

Fig. 4. Day and night "average" wet refractivity profiles

D. The Callahan Model

In late 1973, P. S. Callahan derived a model to predict wet zenith range refraction, as follows (see Ref. 7):

$$\Delta R_{tw} = 10^{-1} C_1 C_3 PW_s \frac{\exp(a^2/4b)}{T_s^2\sqrt{b}}$$

$$\left\{\left(1+\frac{\gamma a}{2T_s b}\right)\frac{\sqrt{\pi}}{2}\left[\operatorname{erf}\left(\sqrt{b}\,H+\frac{a}{2\sqrt{b}}\right)\right.\right.$$

$$\left.-\operatorname{erf}\left(\frac{a}{2\sqrt{b}}\right)\right]+\frac{\gamma}{T_s\sqrt{b}}\left[\exp\left(-\frac{a^2}{4b}\right)\right.$$

$$\left.\left.-\exp\left\{-\left(\sqrt{b}\,H+\frac{a}{2\sqrt{b}}\right)^2\right\}\right]\right\}$$

where

$\frac{1}{a} = 1.4 + 0.078\,T_s\,(°C)$; fit parameter

$\frac{1}{b} = 8.7 + 0.43\,T_s\,(°C)$; fit parameter

H = height at which water vapor vanishes

$$\operatorname{erf}(x) = \frac{2}{\sqrt{\pi}}\int_0^x \exp(-y^2)\,dy$$

The basis of this model was an empirical fit to water vapor pressure (data from western Europe) in the form of

$$PW(z) = PW_s \exp(-az - bz^2)$$

in addition to the use of a constant lapse rate temperature:

$$T(z) = T_s - \gamma z$$

which, when combined, simply yields

$$\Delta R_{tw} = 10^{-1} C_1 C_3 \int_0^H \frac{PW_s \exp(-az - bz^2)}{(T_s - \gamma z)^2}\,dz$$

The model in its full form is rather awkward; Callahan indicates that for the following nominal values:

$a = 0.248\ \text{km}^{-1}$

$b = 0.048\ \text{km}^{-1}$

$\gamma = 7\ \text{K/km}$

$H = 10\ \text{km}$

$T = 300\ \text{K}$

The model reduces to ("Callahan")[1]

$$\Delta R_{tw} = \frac{1.15 \times 10^{-2} PW_s}{(T_s/300)^2}$$

This model, now to be called "Callahan," is compared to the Appendix A test cases in Table 3.

[1]It is to be understood that the model loses accuracy for T_s outside the range $200\ \text{K} < T_s < 310\ \text{K}$.

Table 3. Callahan vs Actual

Case No.	Callahan, cm	Actual, cm	Δ, cm
Night cases			
1	3.8	4.8	−1.0
3	4.1	3.8	+0.3
5	3.2	3.7	−0.5
7	15.4	18.1	−2.7
9	4.8	9.7	−4.9
Day cases			
2	2.6	4.6	−2.0
4	3.7	2.9	+0.8
6	5.0	4.6	+0.4
8	21.2	19.3	+1.9
10	6.5	5.7	+0.8

The statistics of Table 3 are as follows:

$$\sigma_{\text{night}} = 2.6 \text{ cm}$$

$$\sigma_{\text{day}} = 1.3 \text{ cm}$$

$$\sigma_{\text{total}} = 2.0 \text{ cm}$$

$$\text{bias}_{\text{night}} = -1.8 \text{ cm}$$

$$\text{bias}_{\text{day}} = +0.4 \text{ cm}$$

The σ_{day} value can be compared to Callahan's own published day case standard deviation (from Table 2, "All," Ref. 7):

$$\sigma_{\text{day}} = 1.4 \text{ cm}$$

The above results are substantially better than the Chao model in both the standard deviation and the bias; additional analysis of the Callahan model will be presented in Subsection III-F.

E. Empirical Approach to the Prediction of Wet Zenith Range Refraction

In the course of developing a new radio frequency angular tropospheric refraction model (Refs. 8, 9, and 10), this author found it necessary to determine the ratio of wet zenith range refraction to dry zenith range refraction, i.e., to determine some f such that

$$f = \frac{\Delta R_w}{\Delta R_d} = \frac{\int_0^\infty NW(z)\,dz}{\int_0^\infty ND(z)\,dz}$$

At that time it was empirically found that there existed strong correlation between the ratios of wet and dry zenith range refraction and of wet and dry surface refractivity, i.e.,

$$f = \frac{\Delta R_w}{\Delta R_d} \approx K\left[\frac{NW_s}{ND_s}\right]$$

with

$$K \approx 0.32$$

There was an immediate implication that, if indeed, there existed strong correlation, this (assumed) relationship might be useful in predicting wet zenith range refraction.

If

$$\frac{\Delta R_w}{\Delta R_d} \approx K\left[\frac{NW_s}{ND_s}\right]$$

then

$$\Delta R_w \approx K\left[\frac{\Delta R_d}{ND_s}\right] NW_s$$

$$\approx K(RH_s)\left[\frac{6677}{T_s}\right] \exp\left(\frac{AT_s - B}{T_s - C}\right)$$

In 1970, J. V. Ondrasik considered a very similar approach, that is, correlating zenith wet range refraction with surface wet refractivity (Ref. 3, p. 34):

$$\Delta R_w = K_0\,[NW_s] + K_1$$

but (apparently) dropped the idea as unpromising.

The 10 cases in Appendix A were utilized to perform a least squares curve fit to

$$\Delta R_w \text{ vs } K\left[\frac{\Delta R_d}{ND_s}\right] NW_s$$

which resulted in the following value of K:

$$K = 0.3224$$

or, the following model ("Berman 74"):

$$\Delta R_{te} = 2153\left[\frac{RH_s}{T_s}\right]\exp\left(\frac{AT_s - B}{T_s - C}\right)$$

In Table 4, this model is compared to the Appendix A test cases.

The statistics of Table 4 are as follows:

$$\sigma_{night} = 2.6 \text{ cm}$$

$$\sigma_{day} = 1.6 \text{ cm}$$

$$\sigma_{total} = 2.2 \text{ cm}$$

$$\text{bias}_{night} = -1.9 \text{ cm}$$

$$\text{bias}_{day} = +0.6 \text{ cm}$$

As can be seen from a comparison with Table 3, the above model and the Callahan model produce substantially similar results (about which more will be said in the next Subsection).

Since all the models (with the exception of Berman 70) show a very strong negative bias for night cases when compared to day cases, one is motivated to consider the causes of and possible solutions to this difficulty. The main considerations that detract from an "average" wet refractivity profile are fluctuations in relative humidity:

$$RH(z) \neq RH_s$$

and near surface variations in temperature. As has already been commented on, the fluctuations in relative humidity are difficult to categorize, while the near surface temperature undergoes a fairly regular diurnal swing, as can be seen in both Figs. 1 and 2.

If one assumes an "average" wet refractivity profile, then obviously using a "night" NW_s will give too small a total wet zenith range refraction; conversely, using a "day" NW_s will lead to too large a total wet zenith refraction, as is (schematically) seen in Fig. 4.

The conclusion one expects is that the $K(= 0.3224)$ determined for a mixture of day and night cases would be larger for night only cases and smaller for day only

Table 4. Berman 74 vs Actual

Case No.	Berman 74, cm	Actual, cm	Δ, cm
Night cases			
1	3.5	4.8	−1.3
3	3.8	3.8	0.0
5	3.1	3.7	−0.6
7	15.5	18.1	−2.6
9	4.6	9.7	−5.1
Day cases			
2	2.5	4.6	−2.1
4	3.6	2.9	+0.7
6	5.1	4.6	+0.5
8	21.9	19.3	+2.6
10	6.8	5.7	+1.1

profiles. This in fact turns out to be the case. Once again, a model with the following form is postulated:

$$\Delta R_{te} = K(RH_s)\left[\frac{6677}{T_s}\right]\exp\left(\frac{AT_s - B}{T_s - C}\right)$$

where

$$K = \begin{cases} K_d & \text{day profiles} \\ K_n & \text{night profiles} \end{cases}$$

A least squares curve fit was performed on the Appendix A test cases. This process yielded

$$K_d = 0.2896$$

$$K_r = 0.3773$$

or

$$\Delta R_{te} = \begin{cases} 1934\left[\frac{RH_s}{T_s}\right]\exp\left(\frac{AT_s - B}{T_s - C}\right); & \text{day profiles} \\ 2519\left[\frac{RH_s}{T_s}\right]\exp\left(\frac{AT_s - B}{T_s - C}\right); & \text{night profiles} \end{cases}$$

This model ("Berman (D/N)") is compared to the Appendix A test cases in Table 5.

Table 5. Berman (D/N) vs Actual

Case No.	Berman (D/N), cm	Actual, cm	Δ, cm
Night cases			
1	4.1	4.8	−0.7
3	4.4	3.8	+0.6
5	3.6	3.7	−0.1
7	18.1	18.1	0.0
9	5.4	9.7	−4.3
Day cases			
2	2.2	4.6	−2.4
4	3.2	2.9	+0.3
6	4.6	4.6	0.0
8	19.7	19.3	+0.4
10	6.1	5.7	+0.4

The statistics of Table 5 are as follows:

$$\sigma_{night} = 2.0 \text{ cm}$$

$$\sigma_{day} = 1.1 \text{ cm}$$

$$\sigma_{total} = 1.6 \text{ cm}$$

$$\text{bias}_{night} = -0.9 \text{ cm}$$

$$\text{bias}_{day} = -0.3 \text{ cm}$$

As can be seen by comparing the above with Table 4, the separate day-night model represents a definite improvement over the composite model.

As an alternate attempt to explore methods to account for the systematic diurnal surface temperature variations, the following was tried.

Let

$T_{min} \approx$ lowest previous 24-h temperature

$T_{max} \approx$ highest previous 24-h temperature

Then, to moderate the night and day temperature profile distortions, define:

$$T\,(\text{night cases}) = \frac{3T_{min} + T_{max}}{4}$$

$$T\,(\text{day cases}) = \frac{3T_{max} + T_{min}}{4}$$

A new K for the above defined model (now to be called the "Berman (TMOD)") was calculated via least squares as:

$$K = 0.3281$$

This model is compared to the Appendix A test cases in Table 6.

Table 6. Berman (TMOD) vs Actual

Case No.	Berman (TMOD), cm	Actual, cm	Δ, cm
Night cases			
1	4.6	4.8	−0.2
3	4.8	3.8	+1.0
5	4.1	3.7	+0.4
7	17.5	18.1	−0.6
9	6.3	9.7	−3.4
Day cases			
2	2.0	4.6	−2.6
4	2.9	2.9	0.0
6	4.0	4.6	−0.6
8	19.8	19.3	+0.5
10	5.3	5.7	−0.4

The satistics of Table 6 are as follows:

$$\sigma_{night} = 1.6 \text{ cm}$$

$$\sigma_{day} = 1.2 \text{ cm}$$

$$\sigma_{total} = 1.4 \text{ cm}$$

$$\text{bias}_{night} = -0.6 \text{ cm}$$

$$\text{bias}_{day} = -0.6 \text{ cm}$$

As can be seen by comparison with Table 5, the results are exceedingly similar to the separate day-night model, as one would expect because of the similarity in assumptions.

Finally, Subsection III-F will compare the various models discussed in this Section.

F. Comparison of Wet Zenith Range Refraction Models

The results of each of the models previously presented are summarized in Table 7.

Table 7. Composite model comparison

Parameter	Berman 70	Chao	Callahan	Berman 74	Berman (D/N)	Berman (TMOD)
σ_{night}	5.5	3.5	2.6	2.6	2.0	1.6
σ_{day}	1.4	1.9	1.3	1.6	1.1	1.2
σ_{total}	4.0	2.8	2.0	2.2	1.6	1.4
$bias_{night}$	+4.4	−3.0	−1.8	−1.9	−0.9	−0.6
$bias_{day}$	−0.6	−0.5	+0.4	+0.6	−0.3	−0.6

Additionally, the model residuals for the test cases are seen in Figs. 5 and 6, while Fig. 7 compares the Chao, Callahan, and Berman 74 model for $RH_s = 0.3$ and a temperature range of 270 K to 310 K.

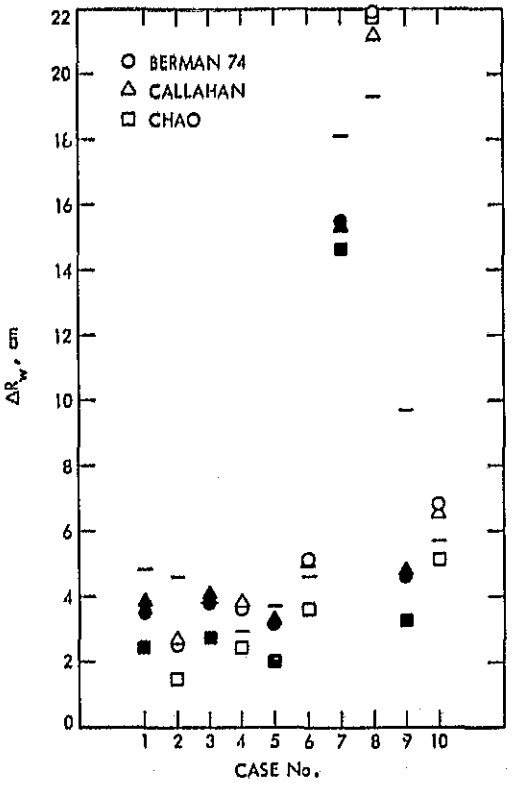

Fig. 5. Test case comparison of the Berman 74, Callahan, and Chao models

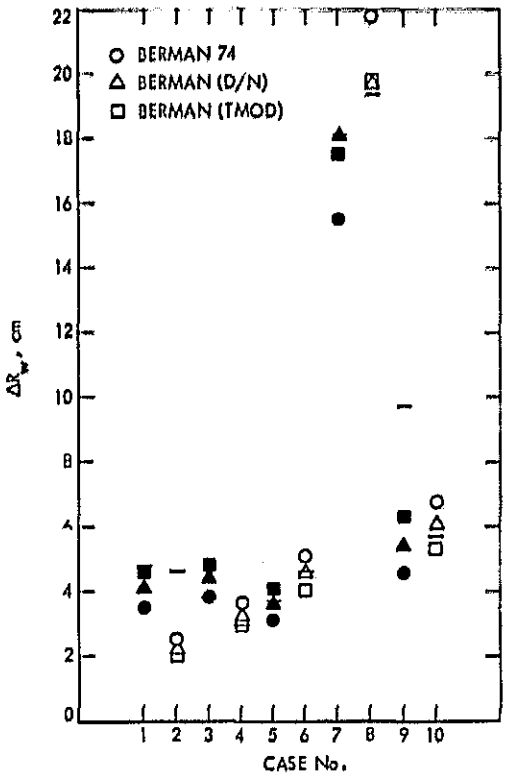

Fig. 6. Test case comparison of the Berman 74, Berman (D/N), and Berman (TMOD) models

The models can be characterized as follows:

(1) Berman 70: day cases work reasonably well, but night cases are totally useless, primarily because of relatively high near surface relative humidity and strong nighttime temperature inversions, both of which combine to cause the model to yield excessively high values.

(2) Chao: day case experience is reasonably good, but night cases show a high standard deviation. Even more troublesome, the entire model has a negative bias, small for the day cases, but very large for the night cases (this is readily apparent by examining Fig. 7).

(3) Callahan: day case experience is very good and night cases work reasonably well. Night cases still show a substantial negative bias, however.

(4) Berman 74: the results of this model are very similar to those obtained with the Callahan models. That these two models are very similar can be seen in Fig. 7; however, this similarity is not surprising if the models are put in the same form:

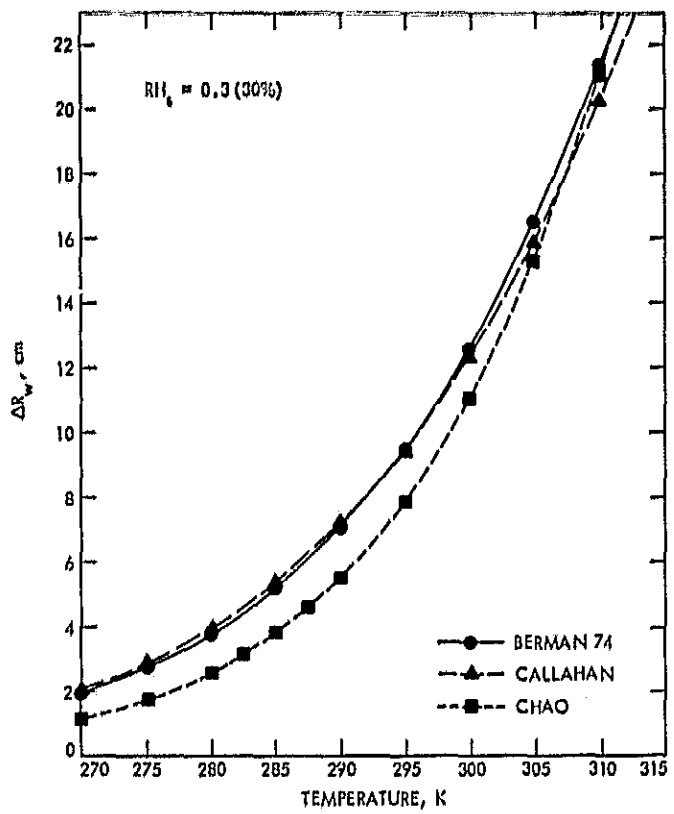

Fig. 7. Comparison of the Berman 74, Callahan, and Chao models

Callahan:

$$\Delta R_{te} = \frac{1.15 \times 10^{-2} PW_s}{(T/300)^2}$$

and Berman 74:

$$\Delta R_{te} = \frac{1.18 \times 10^{-2} PW_s}{(T/300)}$$

The difference (in cm) between $(T/300)^{-1}$ and $(T/300)^{-2}$ only becomes significant at very high surface temperatures ($T_s \gtrsim 305$ K).

(5) Berman (D/N): very good experience is obtained with both day and night cases. This model is similar in form to both the Callahan and Berman 74 models, except that it has separate coefficients for night versus day cases to make allowances for the qualitatively known effects due to diurnal temperature fluctuations. In Ref. 6, Chao presented a large data base of ΔR_{te} versus PW_s measured at local noon and at three locations:

(1) Madrid, Spain

(2) Yucca Flats, Nevada

(3) Wagga, Australia

By assuming fixed relative humidity levels one can make a rough comparison of the various models here described. Appendix B displays this data for the following models:

(1) Chao

(2) Berman (D/N); day coefficient

(3) Callahan

and for the following relative humidity levels:

(1) 15.0%

(2) 22.5%

(3) 30.0%

(4) 37.5%

(5) 45.0%

As an example, for the $RH = 30.0\%$ case (Fig. B-3 of Appendix B), the models yielded the following statistics when passed through the data:

Parameter	Berman (D/N)	Chao	Callahan
σ_{day}, cm	2.06	2.22	2.30
bias_{day}, cm	+0.13	−0.33	+0.99

The above results tend to qualitatively substantiate the model descriptions previously presented in regard to these models.

(6) Berman (TMOD): very similar assumption to the Berman (D/N) model and very similar results in all respects.

At this time, the best choice for an overall model, when considering standard deviation, bias, and complexity, would appear to be the Berman (D/N):

$$\Delta R_{te} = \begin{cases} 1934 \left[\frac{RH_s}{T_s}\right] \exp\left(\frac{AT_s - B}{T_s - C}\right); & \text{day profiles} \\ 2519 \left[\frac{RH_s}{T_s}\right] \exp\left(\frac{AT_s - B}{T_s - C}\right); & \text{night profiles} \end{cases}$$

Finally, it should be pointed out that all the models described here (with the exception of the Chao model) can be put in a very similar form, i.e., if

$$\Delta R_{te} = PW_s \left[A_0 + \frac{A_1}{(T_s/300)} + \frac{A_2}{(T_s/300)^2} \right]$$

one would have for each of the following models:

(1) Berman 70 (with T_s for T_s):

$A_0 = 1.33 \times 10^{-2}$

$A_1 = -0.34 \times 10^{-2}$

$A_2 = +0.02 \times 10^{-2}$

(2) Callahan:

$A_0 = 0$

$A_1 = 0$

$A_2 = 1.15 \times 10^{-2}$

(3) Berman 74:

$A_0 = 0$

$A_1 = 1.18 \times 10^{-2}$

$A_2 = 0$

(4) Berman (D/N):

$A_0 = 0$

$A_1 = 1.06 \times 10^{-2}$ (day); 1.38×10^{-2} (night)

$A_2 = 0$

(5) "Chao Integrated Average Refractivity Profile" (see Refs. 9, 10, 11, and 12)[2]:

$A_0 = 0$

$A_1 = 0$

$A_2 = 1.08 \times 10^{-2}$

(6) "Winn, et. al" (see Ref. 13)[2]:

$A_0 = 0.80 \times 10^{-2}$ (footnote 3)

$A_1 = 0$

$A_2 = 0$

IV. Summary

At the current time the most accurate zenith range refraction model would be composed of the integrated dry refractivity (from Section I) and the Berman (D/N) wet zenith range refraction model, as follows:

(1) Day usage:

$$\Delta R = 10^{-1} C_1 P_s \left(\frac{R}{g}\right) + 1934 \left[\frac{RH_s}{T_s}\right] \exp\left(\frac{AT_s - B}{T_s - C}\right)$$

(2) Night usage:

$$\Delta R = 10^{-1} C_1 P_s \left(\frac{R}{g}\right) + 2519 \left[\frac{RH_s}{T_s}\right] \exp\left(\frac{AT_s - B}{T_s - C}\right)$$

The integrated dry refractivity is (close to) exact, while the wet model accuracy is considered to be:

$$\sigma \sim 1.5 - 2.0 \text{ cm}$$

Possible improvements to the above model (wet portion only) are as follows:

(1) Use of the Callahan functional form ($K[NW_s]$) with corrections for diurnal temperature effects.

Since the most successful (wet) models have been strictly empirical, it would rather straightforwardly seem that a linear proportionality to refractivity would be the most appropriate, i.e., consider:

$$\Delta R_w = 10^{-1} \int_0^H NW(z)\, dz$$

$$= 10^{-1} NW_s \left\{ \int_0^H \frac{NW(z)}{NW_s}\, dz \right\}$$

where

$$\frac{NW(0)}{NW_s} = 1$$

and

$$\frac{NW(H)}{NW_s} = 0$$

Since one, in essence, has no other information, then the quantity

$$\left\{ \int_0^H \frac{NW(z)}{NW_s}\, dz \right\}; \qquad \text{fit parameter}$$

simply becomes the fit parameter, leading to the Callahan form. However, it is also conceivable that something more (empirically) representative of the data might be obtained by allowing more fit parameters in terms of the dominant variable, T_s, in

[2]These two previously mentioned expressions have been added for the sake of comparison.

[3]As a side light, this coefficient is about 30% smaller than more frequently used data from (inland) tracking sites. It is conjectured that this is a result of taking surface measurements at times when a near surface, high relative humidity marine layer was existent.

which case it might be useful to attempt a fit in the form:

$$\Delta R_{tc} = PW_s \left\{ A_0 + \frac{A_1}{(T_s/300)} + \frac{A_2}{(T_s/300)^2} \right\}$$

where A_0, A_1, and A_2 are fit parameters.

(2) Correction for systematic diurnal, seasonal and local (site) effects.

The separate day and night coefficient model (Berman (D/N)) is a step in this direction; ultimately one could visualize fitting to the following parameters:

(1) T_{GMT} = time of day (diurnal)

(2) T_{DOY} = time of year (seasonal)

(3) Tracking station location (l)

so that a complete model could be represented as:

$$\Delta R_{tc} = PW_s \left[\sum_{j=0}^{2} \frac{A_{lj}(T_{GMT}, T_{DOY})}{T_s^j} \right]$$

Even with the above model, this author considers that the information content inherent in surface measurements would not allow the standard deviation of a surface meteorological measurements model to improve to any better than:

$$\sigma \sim 1.0 - 1.5 \text{ cm}$$

as compared to the standard deviation of the best current models of:

$$\sigma \sim 1.5 - 2.0 \text{ cm}$$

Definition of Symbols

A	7.4475 ln (10) = 17.1485	j	index variable
A_j	series coefficients	K, K_j	constants
a	coefficient, empirical water vapor pressure function	l	length
B	2034.28 ln (10) = 4684.1	$N(z)$	total refractivity
B_1	"inverse scale height," km	N_s	$N(0)$
b	coefficient, empirical water vapor pressure function	$ND(z)$	"dry" refractivity
C	38.45	ND_s	$ND(0)$
C_1	0.776	$NW(z)$	"wet" refractivity
C_2	$610\,C_3 = 2934100$	NW_s	$NW(0)$
C_3	4810	$n(z)$	index of refraction
c	speed of light	$P(z)$	total atmospheric pressure, N/m²
F	intermediate variable	P_s	$P(0)$
f	intermediate variable	$PW(z)$	water vapor pressure, N/m²
g	gravitational acceleration	PW_s	$PW(0)$
H	height at which water vapor disappears	R	perfect gas constant
h_0	station height above sea level	RW	perfect gas constant, water vapor

$RH(z)$	relative humidity (100% = 1.0)
RH_s	$RH(0)$
ΔR	range refraction, cm
ΔR_d	"dry" range refraction
ΔR_w	"wet" range refraction
ΔR_θ	range refraction at elevation = θ
r	range, km
r'	refracted range, km
$T(z)$	temperature, K
T_1	216.65 K
T_s	$T(0)$
T_x	extrapolated surface temperature
T_{max}	maximum 24-hour temperature
T_{min}	minimum 24-hour temperature
t	time
v	velocity
W	intermediate variable
Y	variable $(AC - B)/(T - C)$
Y_n	constant $(AC - B)/C$
z	height above station
β	specific heat ratio (1.3 for water vapor)
γ	lapse rate, K/km
θ	elevation angle, deg
ρ	density
ρw	density water vapor
ρ^*	"weighted" density
σ	standard deviation $\left(= \left\{1/N\left[\sum \Delta i^2\right]\right\}^{1/2}\right)$

References

1. Berman, A. L., "A New Tropospheric Range Refraction Model," in *Space Programs Summary*, No. 37-65, Vol. II, pp. 14–15. Jet Propulsion Laboratory, Pasadena, Calif., Sept. 30, 1970.
2. Hess, S. L., *Introduction to Theoretical Meteorology*, Holt, Rinehart & Winston, Inc., New York, 1959.
3. Ondrasik, V. J., and Thuleen, K. L., "Variations in the Zenith Tropospheric Range Effect Computed From Radiosonde Balloon Data," in *The Deep Space Network*, Space Programs Summary 37-65, Vol. II, pp. 25–35. Jet Propulsion Laboratory, Pasadena, Calif., Sept. 30, 1970.
4. Thuleen, K. L., and Ondrasik, V. J., "The Repetition of Seasonal Variations in the Tropospheric Zenith Range Effect," in *The Deep Space Network Progress Report*, Technical Report 32-1526, Vol. VI, pp. 83–98. Jet Propulsion Laboratory, Pasadena, Calif., Dec. 15, 1971.
5. Wu, S. C., "Water-Vapor Range Corrections Above 10,000 Feet Altitude," IOM 391.8-334, December 29, 1975. (JPL internal document.)
6. Chao, C. C., "A New Method to Predict Wet Zenith Range Correction From Surface Measurements," in *The Deep Space Network Progress Report*, No. 32-1526, Vol. XIV, pp. 33–41, Jet Propulsion Laboratory, Pasadena, Calif., April 15, 1973.

7. Callahan, P. S., "Prediction of Tropospheric Wet Component Range Error From Surface Measurements," in *The Deep Space Network Progress Report*, Technical Report 32-1526, Vol. XVIII, pp. 41–46. Jet Propulsion Laboratory, Pasadena, Calif., Dec. 15, 1973.

8. Berman, A. L., and Rockwell, S. T., "A New Angular Tropospheric Refraction Model," in *The Deep Space Network Progress Report 42-24*, pp. 144–164. Jet Propulsion Laboratory, Pasadena, Calif., Dec. 15, 1974.

9. Berman, A. L., and Rockwell, S. T., "A Proposal for a New Radio Frequency Angular Tropospheric Refraction Model For Use Within the DSN," in *The Deep Space Network Progress Report 42-25*, pp. 142–153. Jet Propulsion Laboratory, Pasadena, California, February 15 1975.

10. Berman, A. L., and Rockwell, S. T., *New Optical and Radio Frequency Angular Tropospheric Refraction Models for Deep Space Applications*, Technical Report 32-1601, Jet Propulsion Laboratory, Pasadena, California, November 1, 1975.

11. Berman, A. L., "A New Approach to the Evaluation and Prediction of Wet Tropospheric Zenith Range Refraction" in *The Deep Space Network Progress Report 42-25*, Jet Propulsion Laboratory, Pasadena, California, February 15, 1975.

12. Chao, C. C., "New Tropospheric Range Corrections With Seasonal Adjustment," in *Deep Space Network Progress Report*, No. 32-1526, Vol. VI, pp. 67–73, Jet Propulsion Laboratory, Pasadena, Calif., Dec. 15, 1971.

13. Winn, F. B., et al., "Waterline Radiometer Calibrations Compared to Other Water Vapor Calibration Techniques: Summary of Test Analysis," IOM 391-690, October 2, 1975. (JPL internal document).

Bibliography

Chao, C. C., "Tropospheric Range Effect Due to Simulated Inhomogeneities by Ray Tracing," in *The Deep Space Network Progress Report*, Technical Report 32-1526, Vol. VI, pp. 57–66. Jet Propulsion Laboratory, Pasadena, California, December 15, 1971

Madrid, G. A., et al., "The Tracking System Analytic Calibration Activity for Mariner Mars 1971: Its Function and Scope," in *Tracking System Analytic Calibration Activities for the Mariner Mars 1971 Mission*, Technical Report 32-1587, pp. 1–11. Jet Propulsion Laboratory, Pasadena, California, March 1, 1974.

Miller, L. F., Ondrasik, V. J., and Chao, C. C., "A Cursory Examination of the Sensitivity of the Tropospheric Range and Doppler Effects to the Shape of the Refractivity Profile," in *The Deep Space Network Progress Report*, Technical Report 32-1526, Vol. I, pp. 22–30. Jet Propulsion Laboratory, Pasadena, Calif., Feb. 15, 1971.

Winn, F. B., and Leavitt, R. K., "Refractivity Influence on DSS Doppler Data," in *The Deep Space Network Progress Report*, Technical Report 32-1526, Vol. I, pp. 31–41. Jet Propulsion Laboratory, Pasadena, California, February 15, 1971.

Appendix A

Test Cases

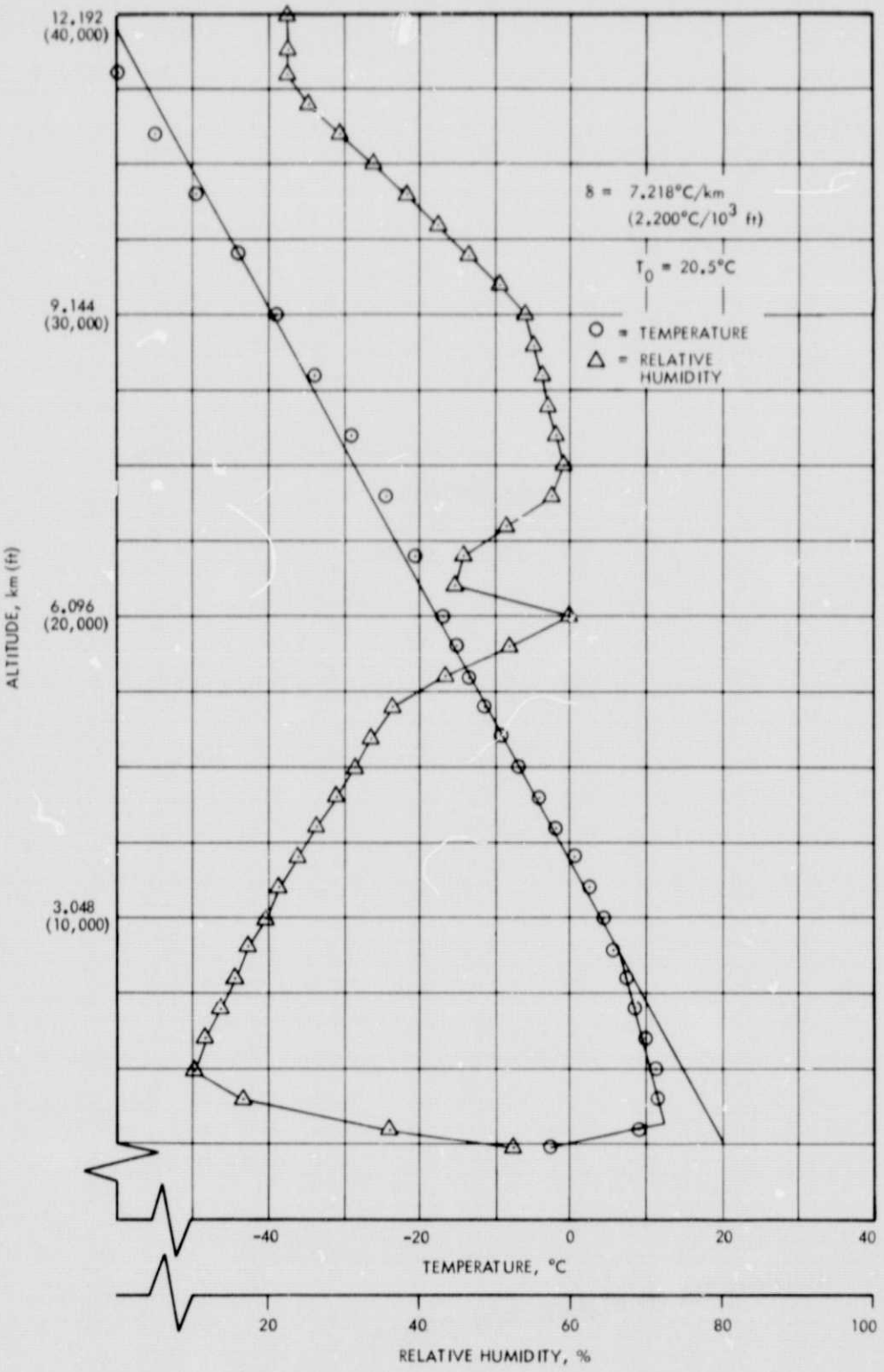

Fig. A-1. Temperature and relative humidity vs altitude; Edwards AFB, December 9, 1968, 2 a.m.

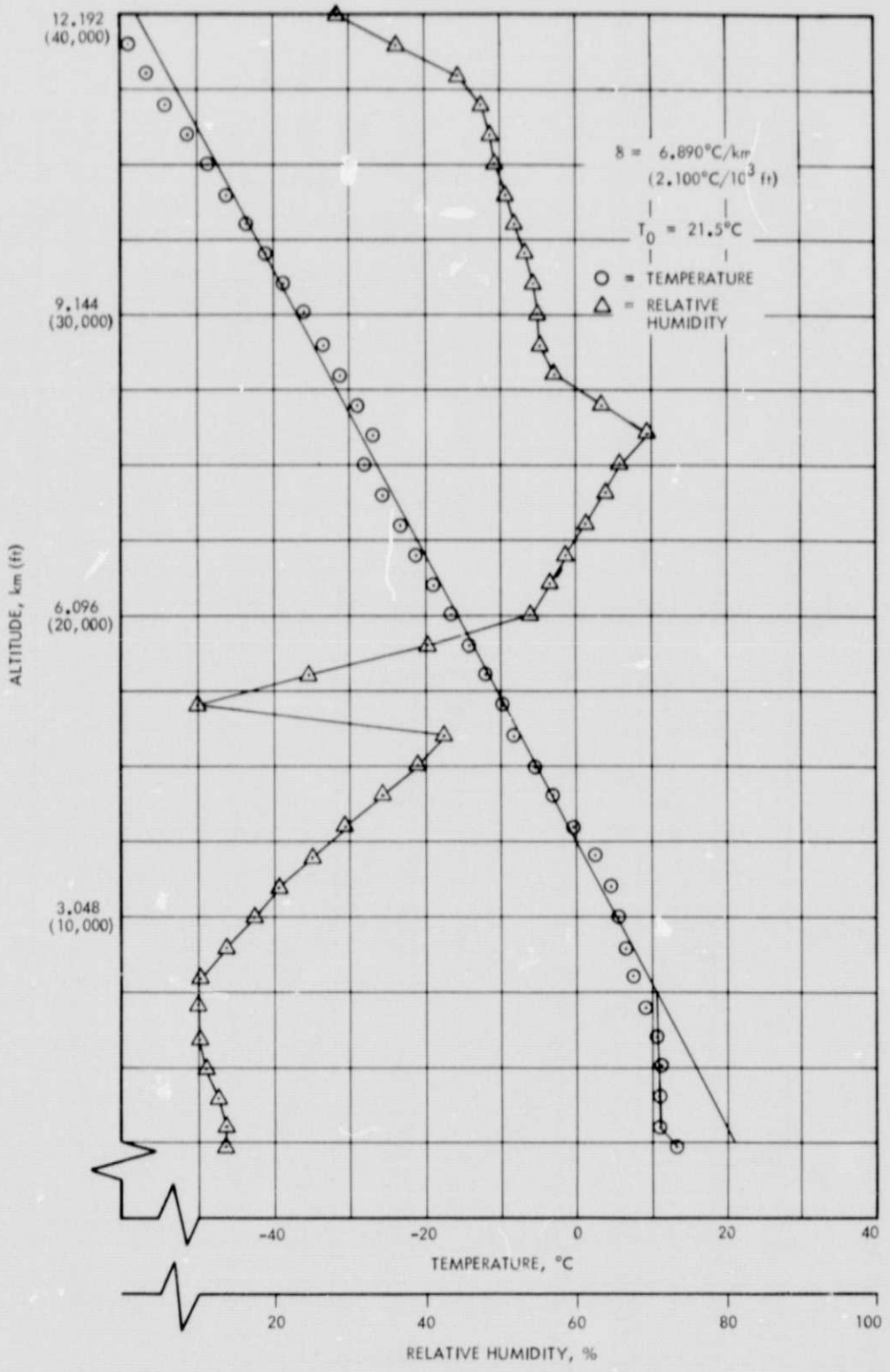

Fig. A-2. Temperature and relative humidity vs altitude; Edwards AFB, December 9, 1968, 1 p.m. local

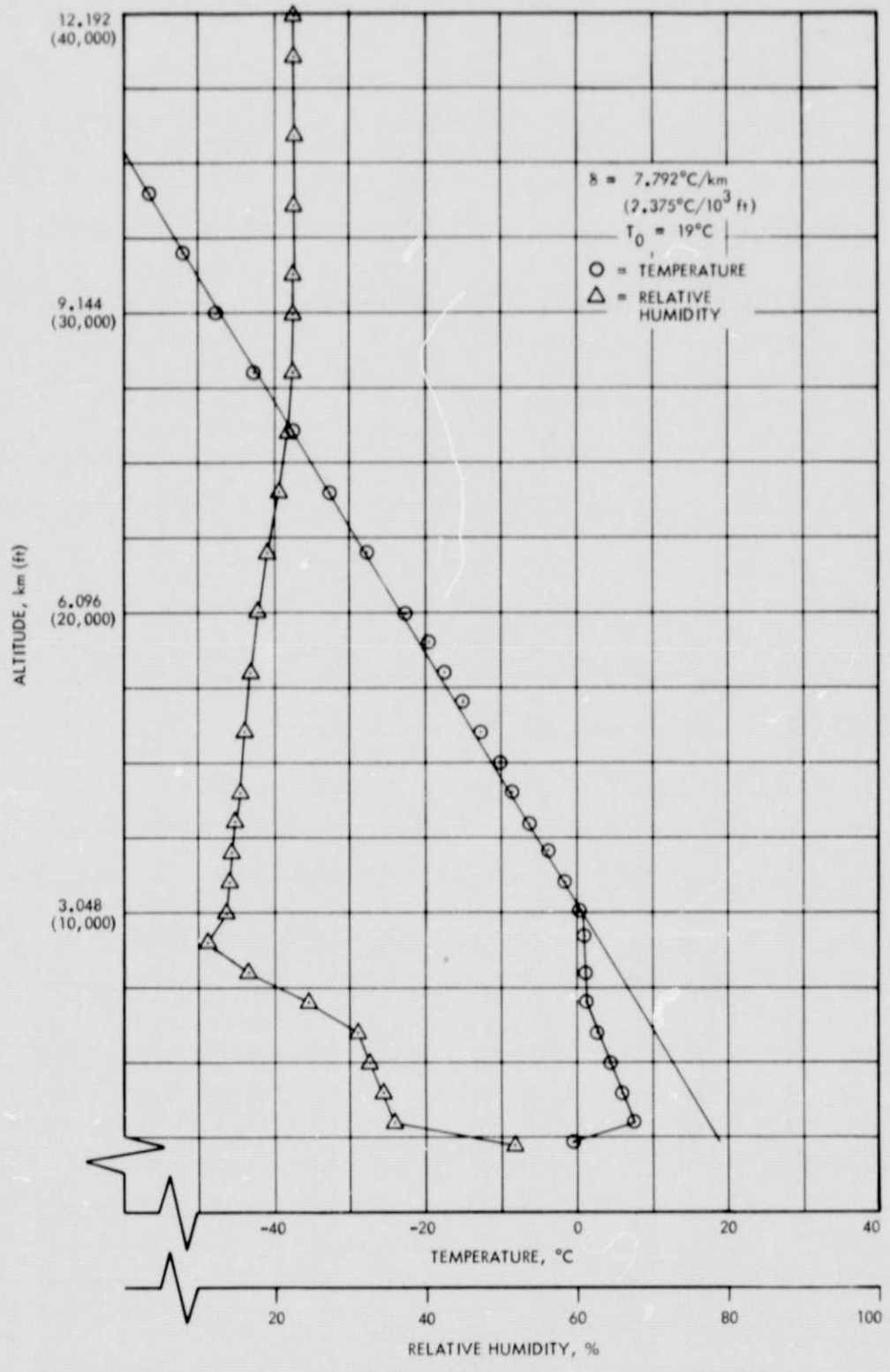

Fig. A-3. Temperature and relative humidity vs altitude; Edwards AFB, February 3, 1969, 2 a.m. local

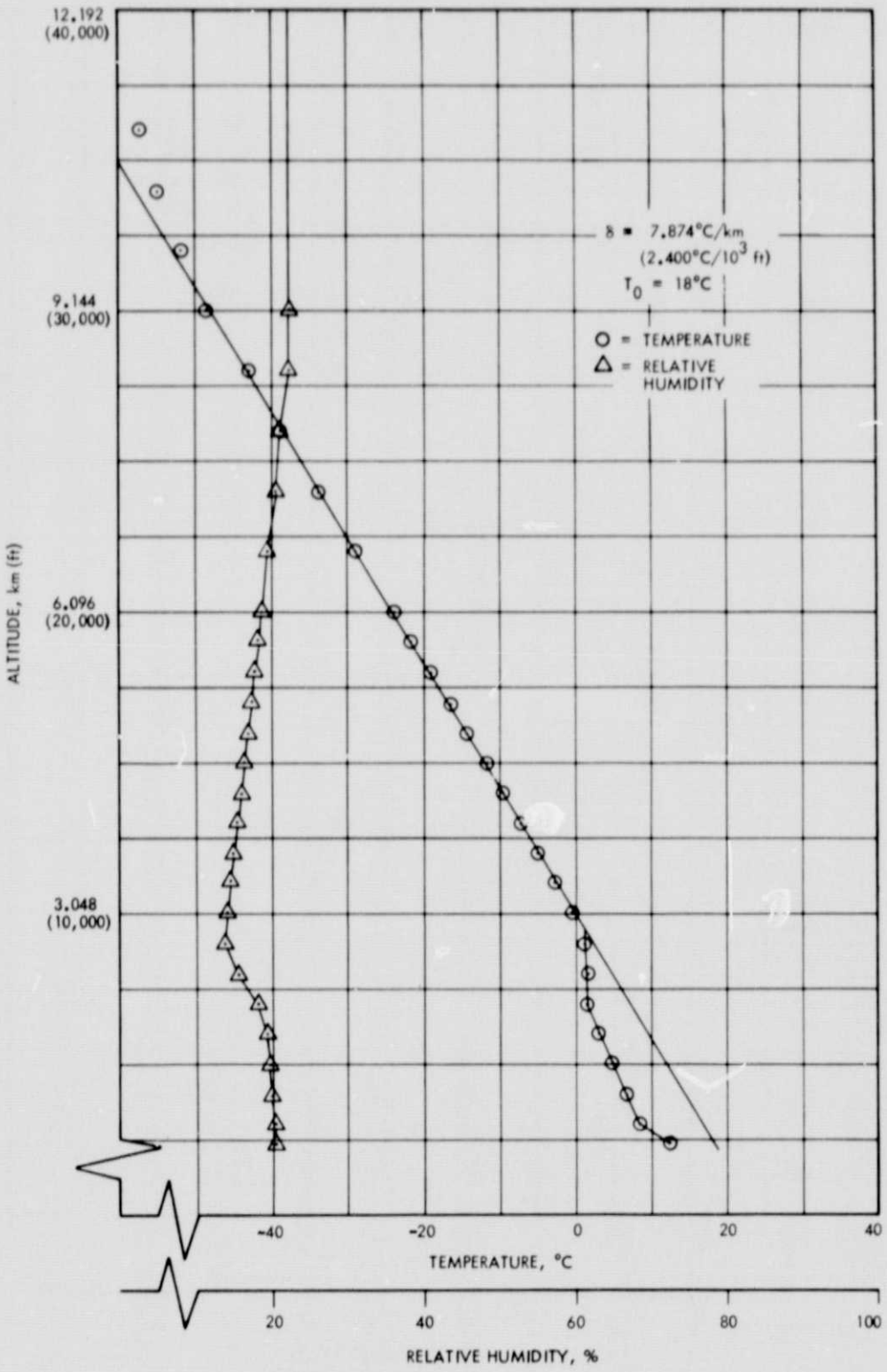

Fig. A-4. Temperature and relative humidity vs altitude; Edwards AFB, February 3, 1969, 1 p.m. local

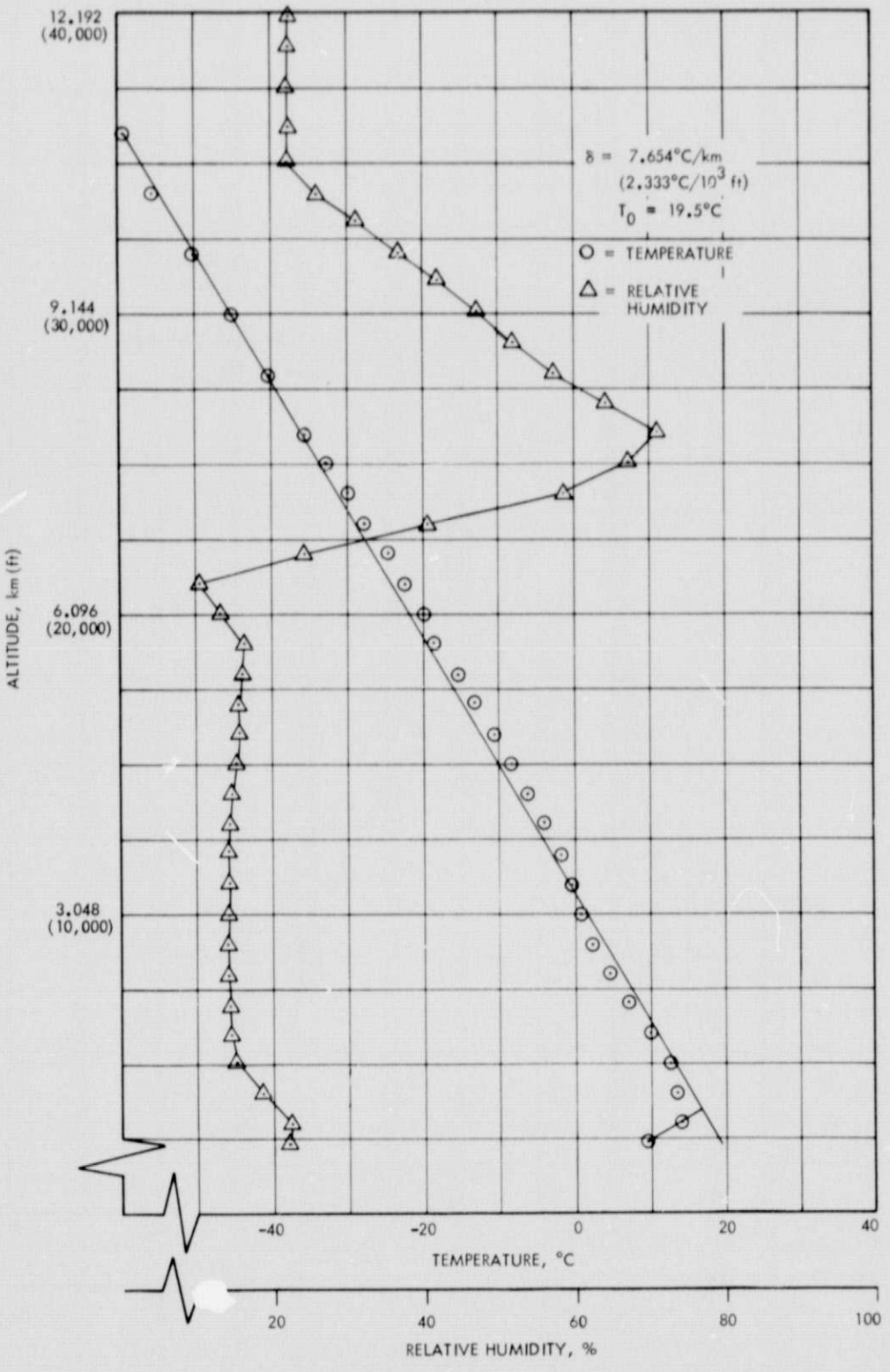

Fig. A-5. Temperature and relative humidity vs altitude; Edwards AFB, April 16, 1969, 12 p.m. local

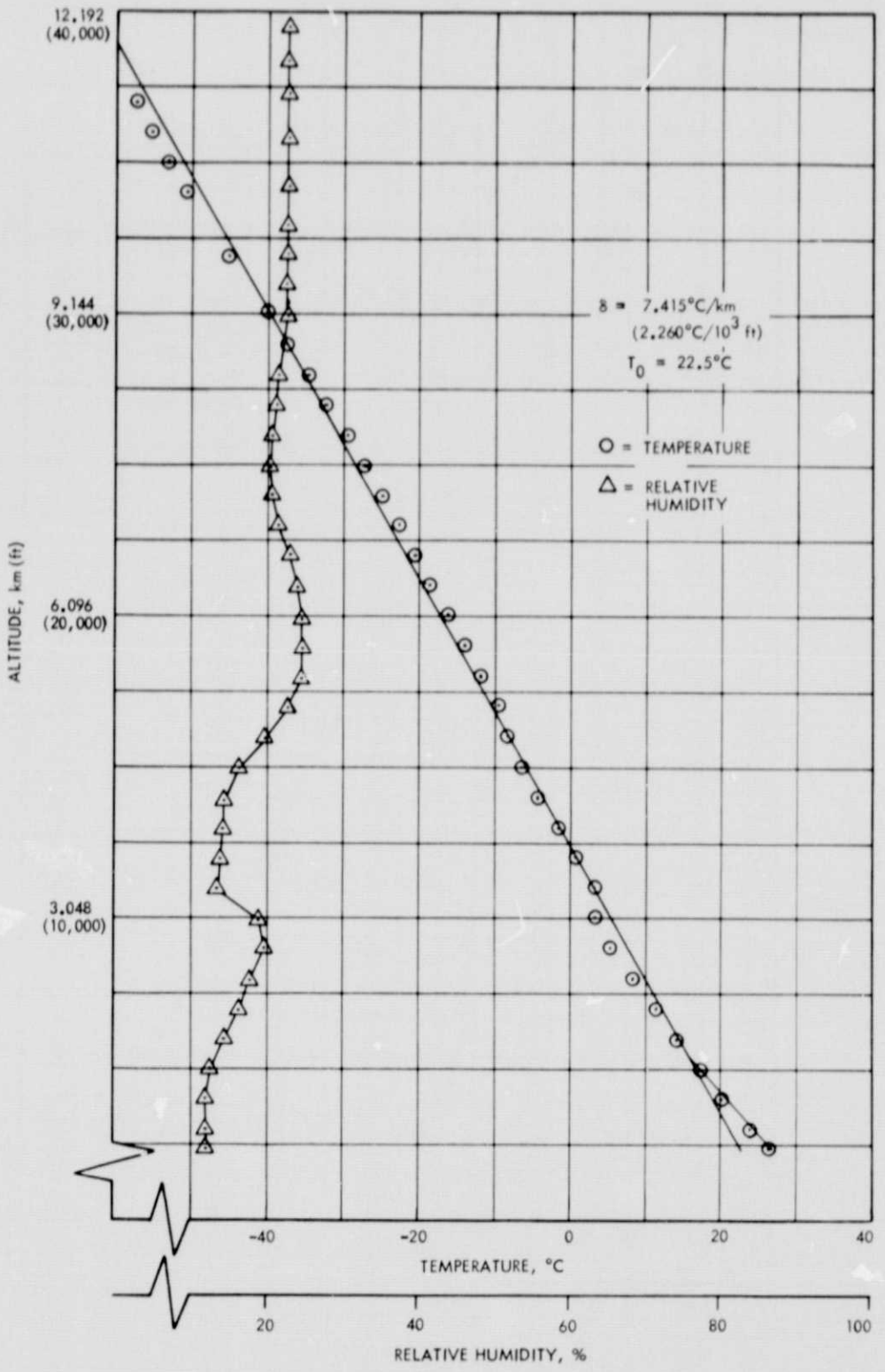

Fig. A-6. Temperature and relative humidity vs altitude; Edwards AFB, April 17, 1969, 2 p.m. local

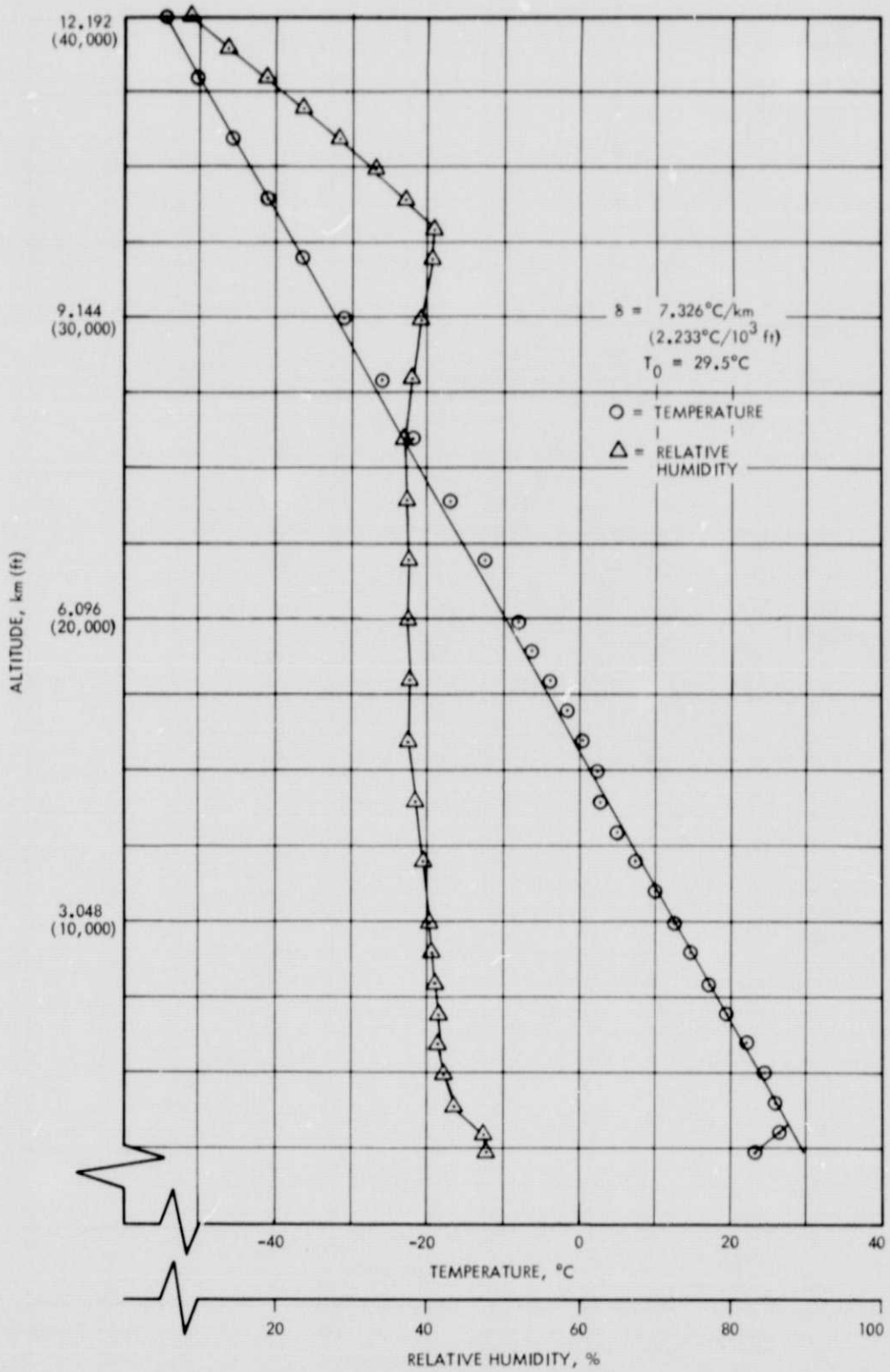

Fig. A-7. Temperature and relative humidity vs altitude; Edwards AFB, August 9, 1969, 1 a.m. local

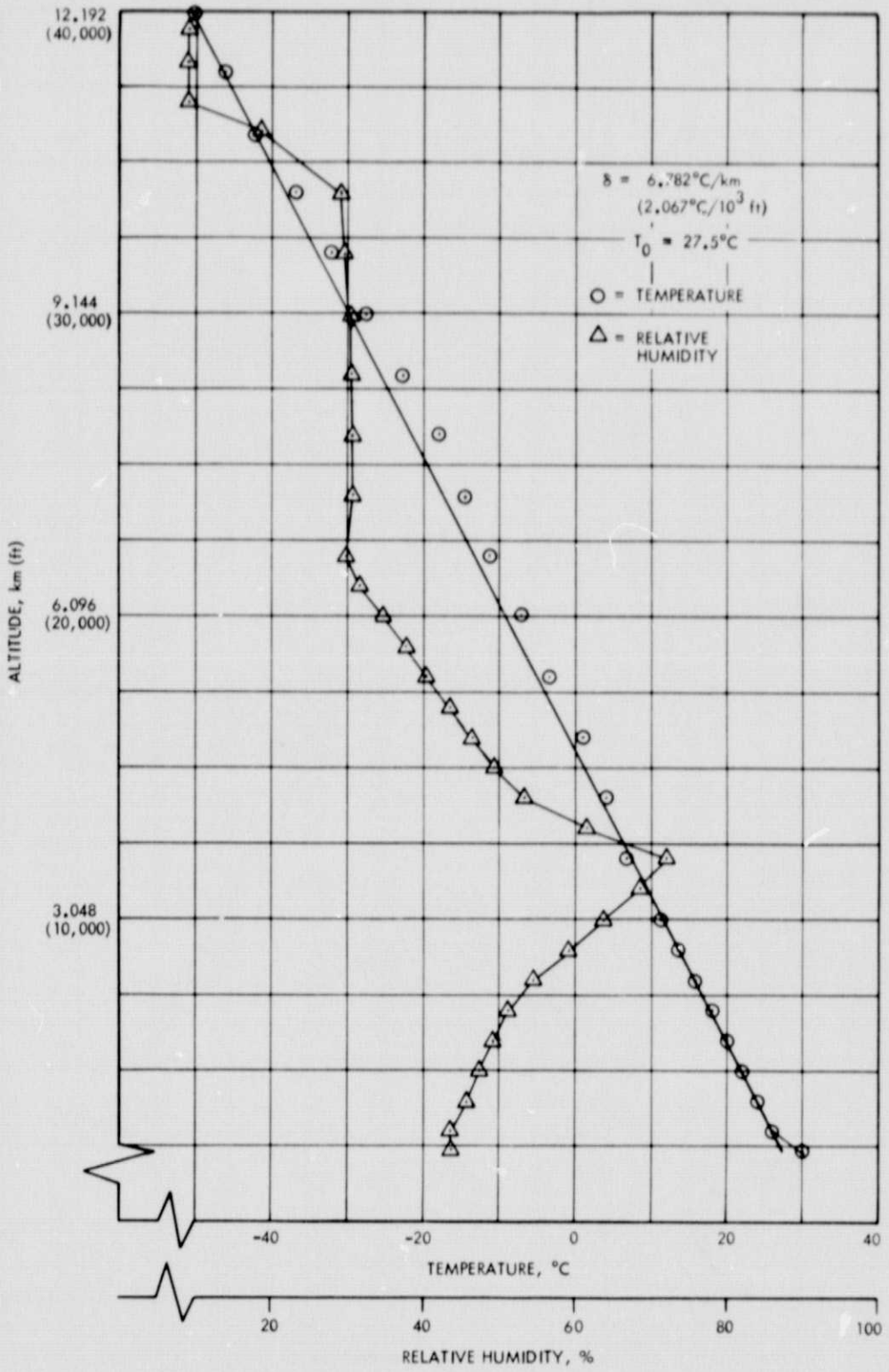

Fig. A-8. Temperature and relative humidity vs altitude; Edwards AFB, August 7, 1969, 10 a.m. local

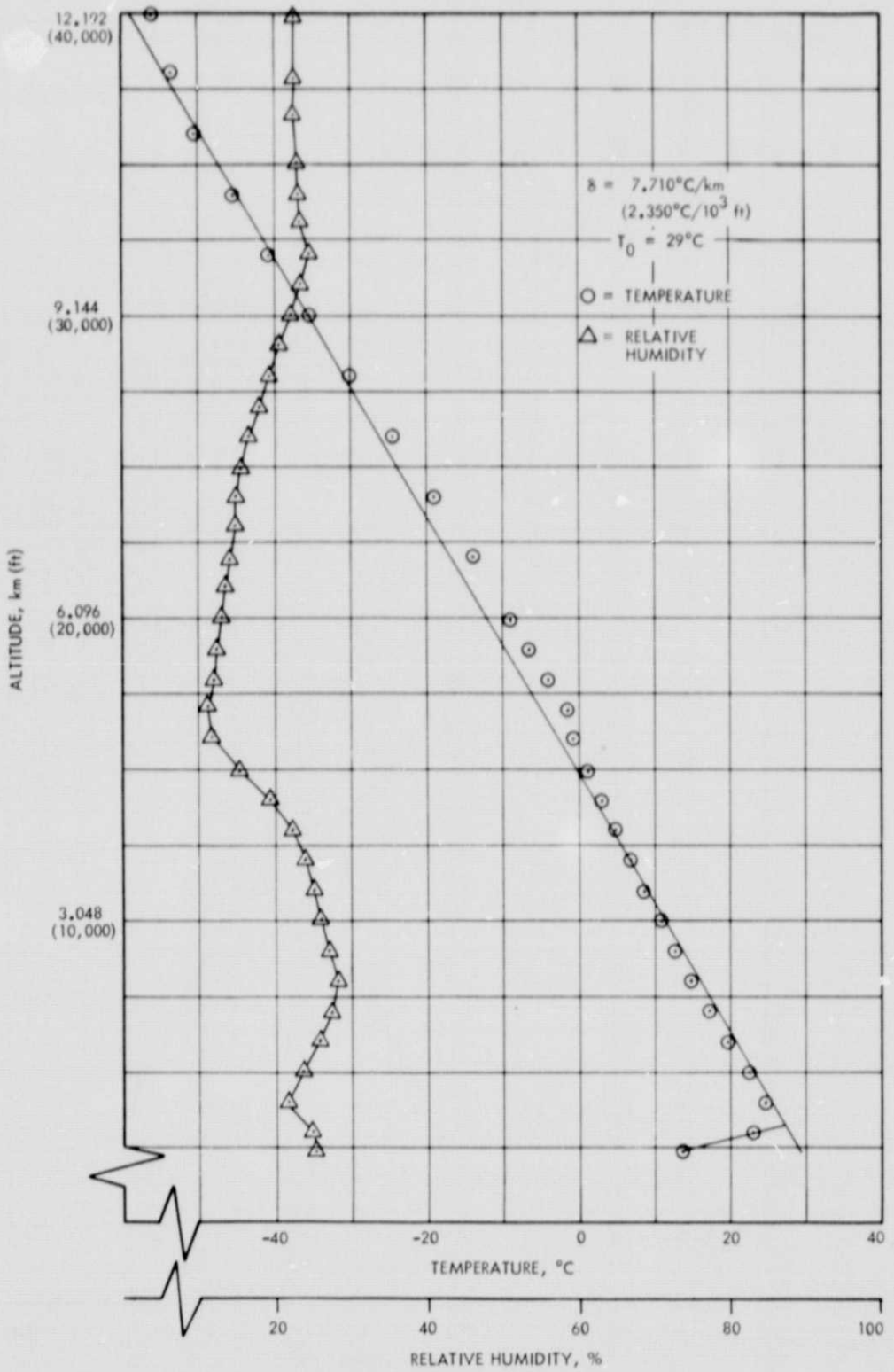

Fig. A-9. Temperature and relative humidity vs altitude; Edwards AFB, September 25, 1968, 1 a.m. local

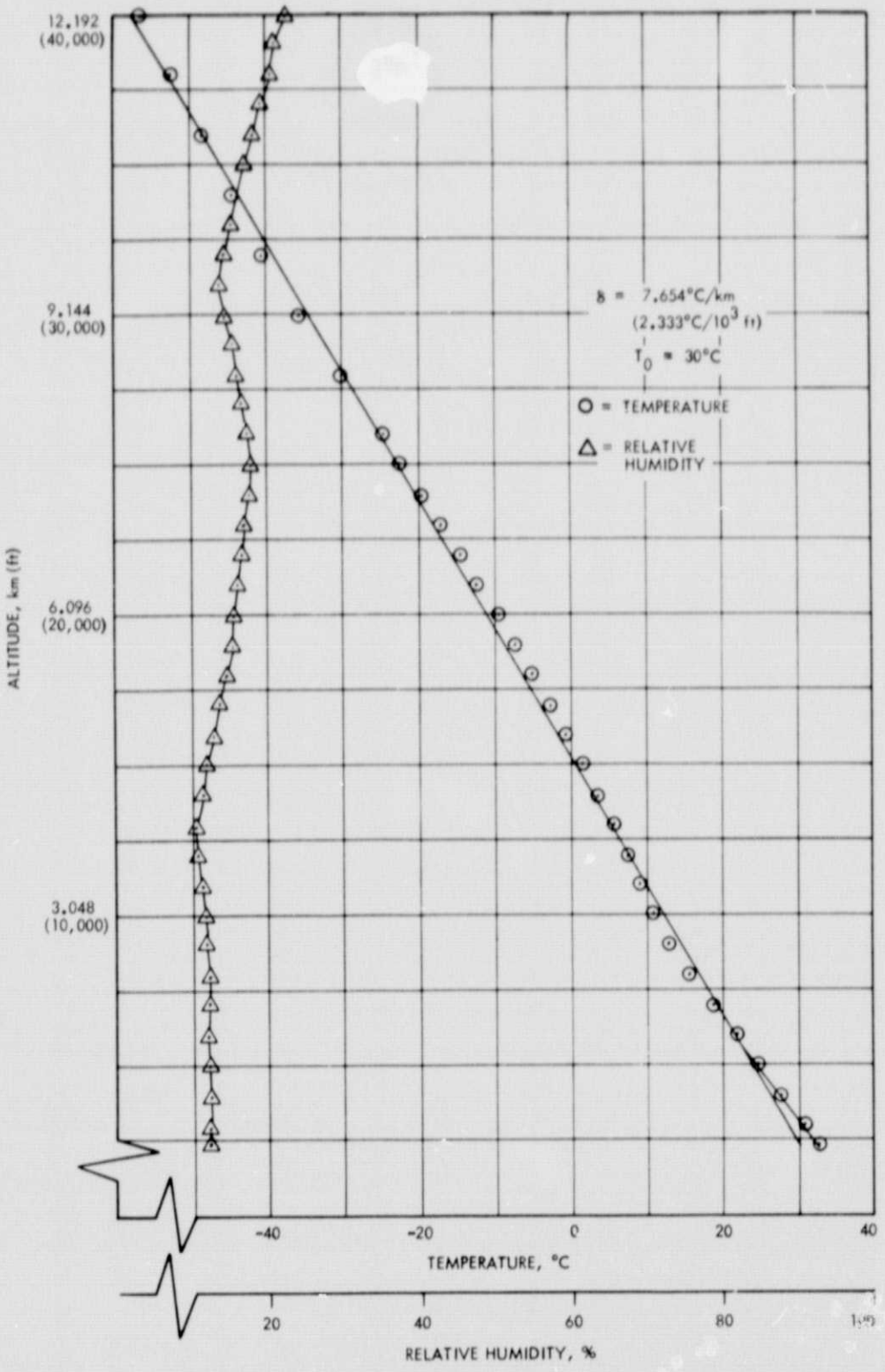

Fig. A-10. Temperature and relative humidity vs altitude; Edwards AFB, September 25, 1968, 12 a.m. local

Appendix B

Model Comparisons to ΔR_w vs PW_s Data

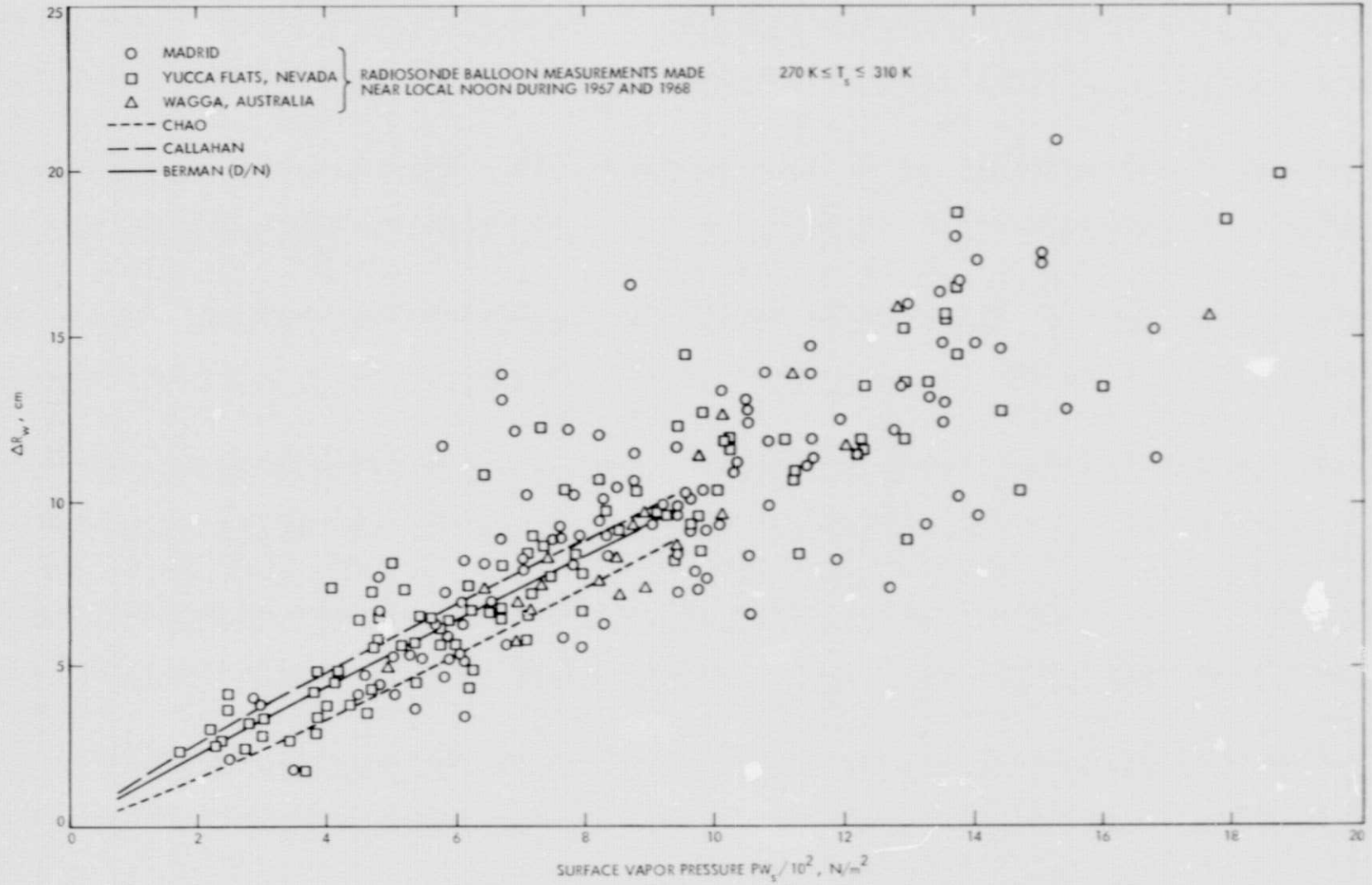

Fig. B-1. Comparison of the Berman (D/N), Callahan, and Chao models for RH_s = 15%

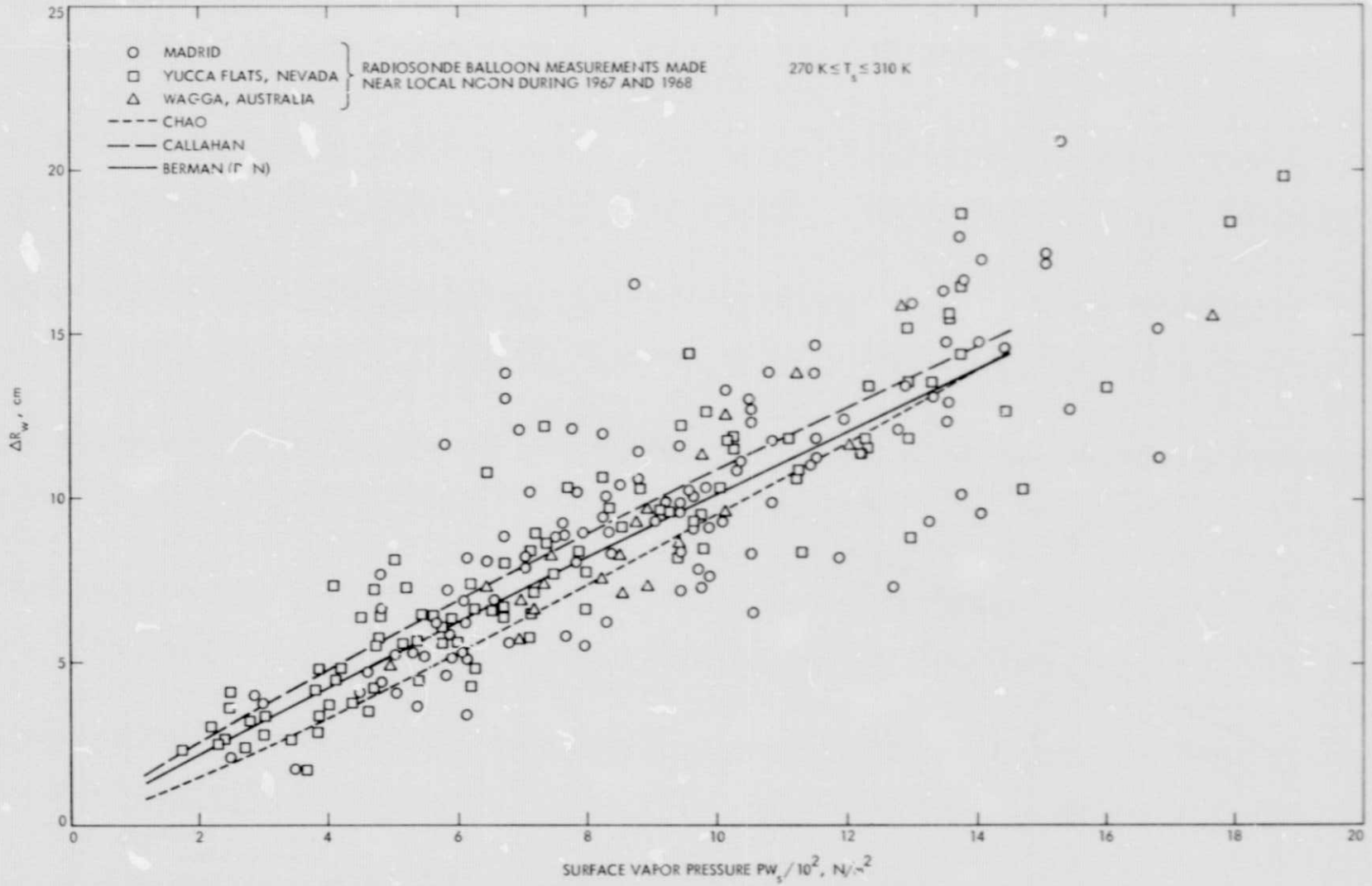

Fig. B-2. Comparison of the Berman (D/N), Callahan, and Chao models for RH_s = 22.5%

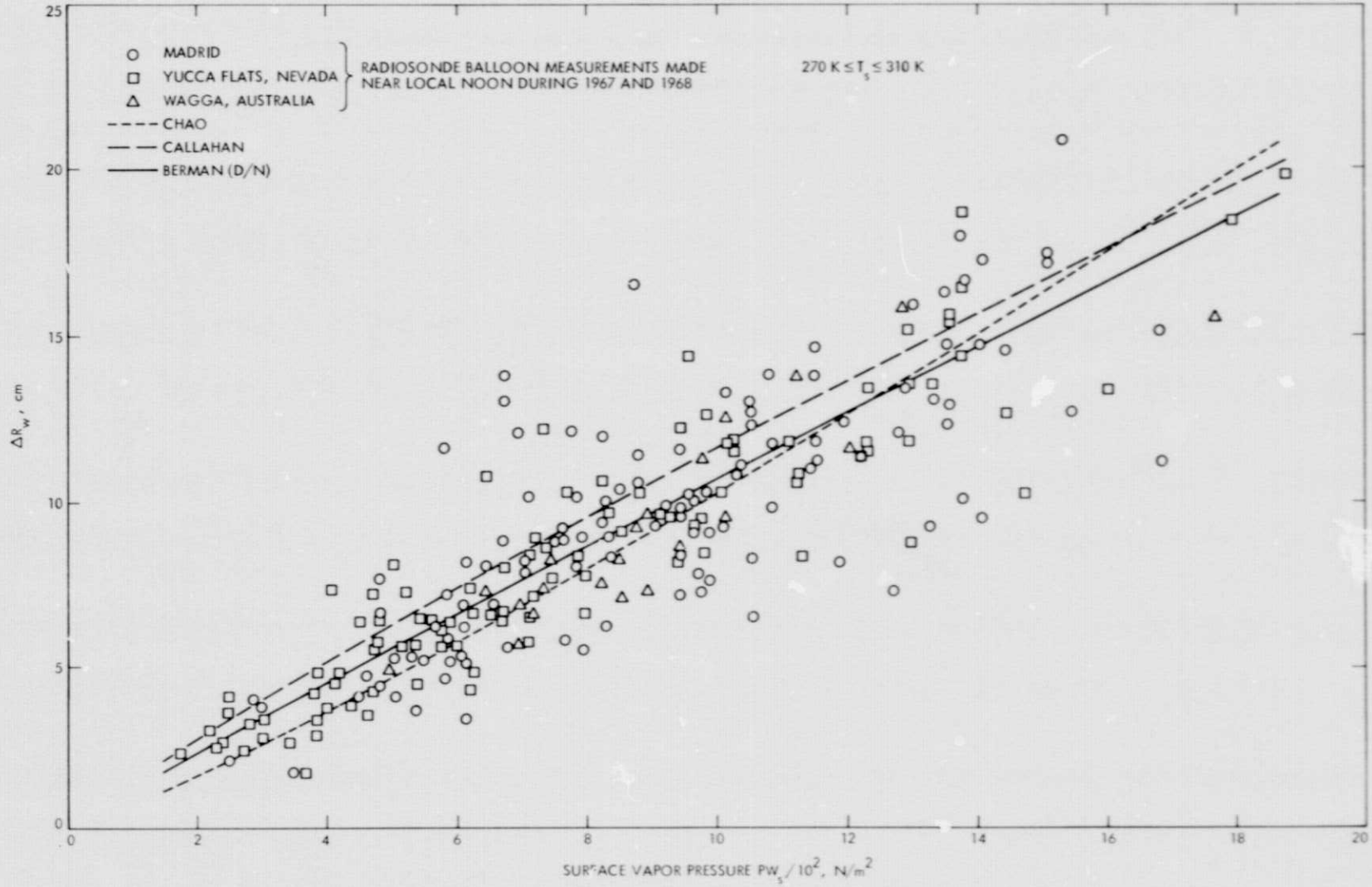

Fig. B-3. Comparison of the Berman (D/N), Callahan, and Chao models for $RH_s = 30\%$

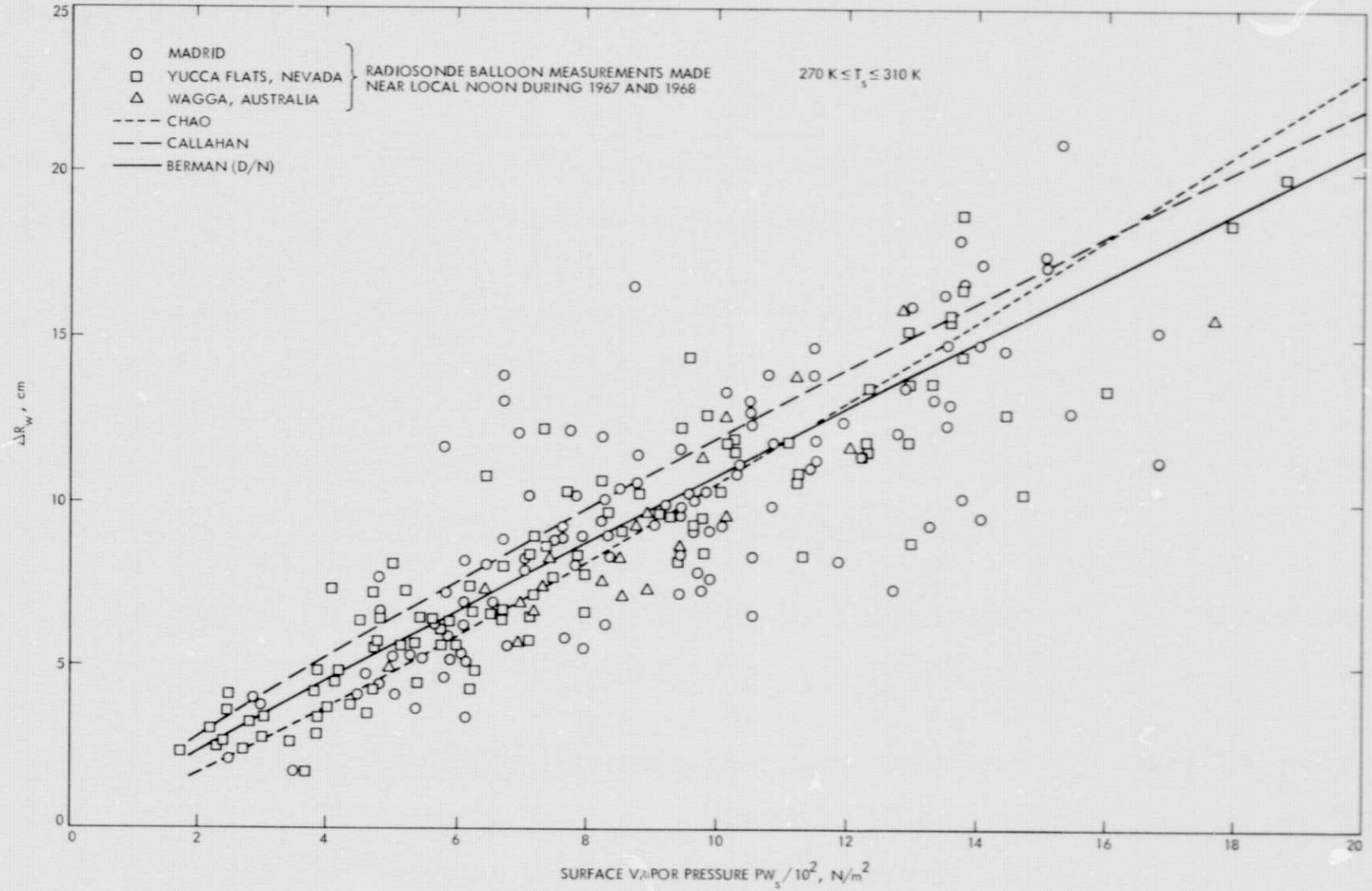

Fig. B-4. Comparison of the Berman (D/N), Callahan, and Chao models for RH_s = 37.5%

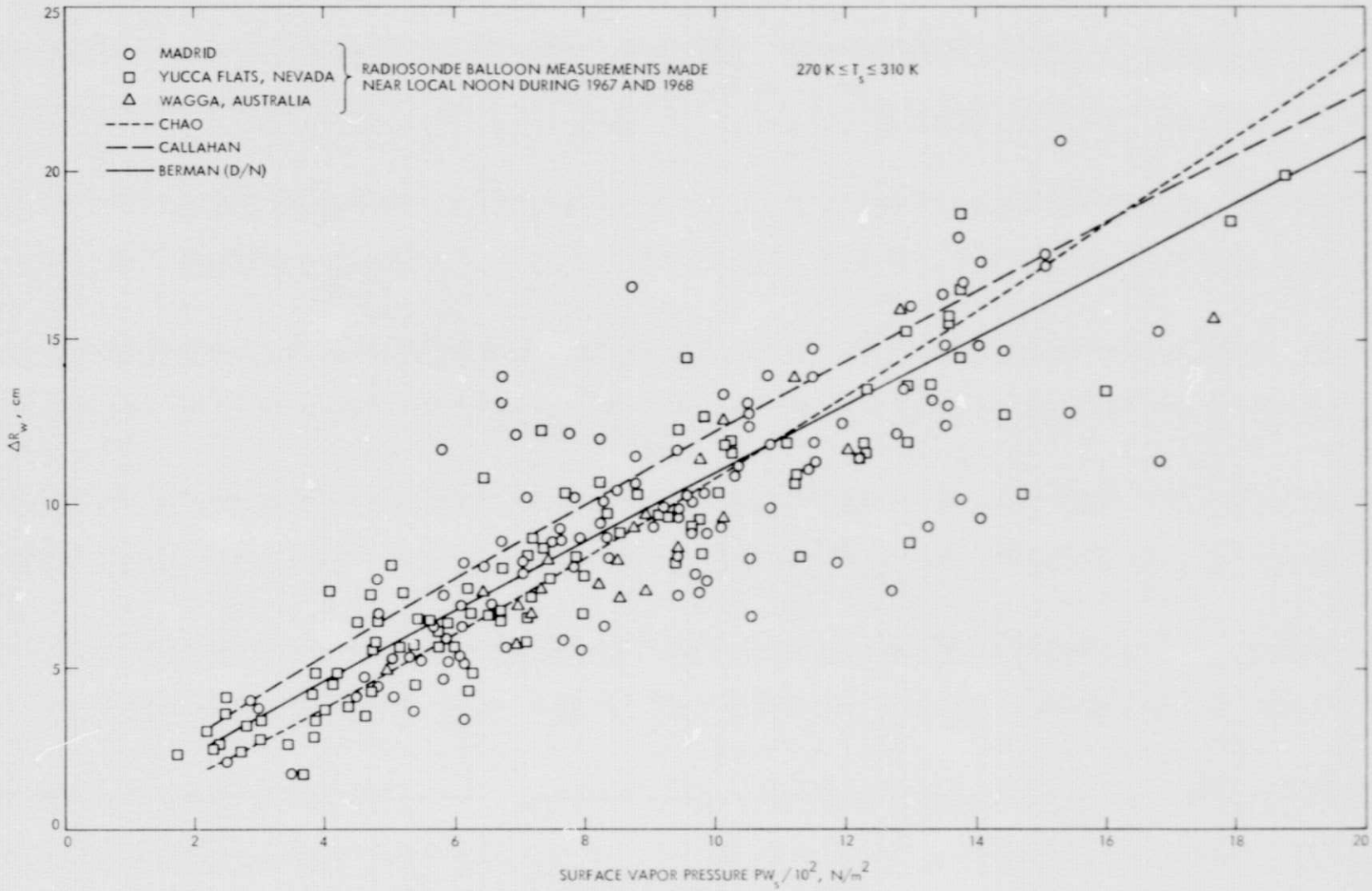

Fig. B-5. Comparison of the Berman (D/N), Callahan, and Chao models for RH_s = 45%

NASA—JPL—Coml., L.A., Calif.